

Università degli Studi di Milano

Facoltà di Scienze e Tecnologie

Corso di Laurea Magistrale in Fisica



MASTER THESIS

Measurement of average Bohmian trajectories of photons
in a double slit interferometer

Internal Supervisor:
Dr. Simone Cialdi

External Supervisor:
Prof. Dr. Harald Weinfurter

Candidate:
Maria Galli
Matr. **884295**

Academic Year 2017-2018

Abstract

Measurement of average Bohmian trajectories of photons in a double slit interferometer

Maria Galli

Chair of Prof. Dr. Hänsch

Research group of Prof. Dr. Harald Weinfurter

Internal supervision of Dr. Simone Cialdi

Bohmian mechanics, a non-local, hidden-variable interpretation of quantum mechanics, allows the description of quantum particle trajectories, otherwise forbidden in the standard approach to quantum mechanics. The non-local character of Bohmian trajectories can be investigated with a pair of entangled photons and a double slit interferometer. The first photon is sent through the double slit apparatus and its trajectories are observed under different measuring conditions chosen for the second photon. The goals of this thesis are the creation of the most crucial part of the experimental setup, i.e. the double slit interferometer, and the measurement of average Bohmian trajectories in the region behind the double slit.

The double-slit setup has been created exploiting the anisotropy of birefringent crystals, which separate a single incoming beam into two beams, orthogonally polarised. In the interference region of this double-slit apparatus, the velocity field of a continuous-wave laser beam has been measured by means of weak measurements. This measurement method allows to extract information from the system leaving it almost unaltered, at the expense of the amount of information extracted. A process of averaging over many such measurements of velocity is therefore required.

Average trajectories of photons have been successfully reconstructed. Their behaviour corresponds to the predictions of Bohmian theory; in particular, the retained interference pattern is evidently recognisable in the density distribution of the observed average trajectories. The significance of average trajectories and the real nature of Bohmian trajectories are still under investigation. With the results achieved in this thesis, the most relevant part of a new experiment is ready to provide further insights on the non-locality of Bohmian mechanics.

Acknowledgements

The realization of this project has been possible and enjoyable because it was shared, professionally and personally, with people that on various fronts and at different times provided their worthy contribution.

Friendly thanks go to Prof. Dr. Harald Weinfurter both for his contagious enthusiasm for scientific research, which made me yearning to write my thesis in his group, and for his personal care of his students. I really appreciated the stimulating, warm and welcoming working environment created also by the other components of the xqp group at LMU München.

In particular, I'm very grateful to Jan Dziejwior and Lukas Knips for their friendly and qualified assistance which made the work pleasant every day. Thanks to Jan for the inspiring and formative conversations, for his daily assistance in any concern and for the positive and smiling attitude towards our work. And thanks to Lukas for generously and patiently sharing his wide knowledge, for his constant availability and his rare attention and kindness with which he took care of my work and my stay.

I'd like to thank also my Italian professors at the Università degli Studi di Milano. Their qualified work and their availability for occasional deeper discussions during my university years let me have the opportunity to build a basis of knowledge and skills for further projects, such as this thesis. In particular, grateful thanks go to Dr. Simone Cialdi, who, with patience, precision and care, introduced me to the world of quantum optics.

I also feel deeply grateful to my parents who always encouraged my personal growth and education. Heartfelt thanks to my sisters, Giulia and Sofia, for their support during those years in any circumstances and for their visits in Munich which made me whole. Grateful thanks to Leonardo for standing by me with affection during this time, making the daily life pleasant and cheerful. To my friends in Italy, especially the ones at the Physics department with which I shared amazing university years, and to my friends in Munich, which made my stays abroad lively and personally enriching.

Finally I acknowledge the Erasmus scholarship, which supported this thesis project and allows students to experience international collaborations at an early stage of their education.

Contents

Abstract	i
Acknowledgments	iii
Introduction	viii
1 Bohmian Mechanics	1
1.1 Problems and limitations in orthodox Quantum Mechanics	1
1.2 Introduction to Bohmian Mechanics	3
1.2.1 An ontological basis for the Quantum Theory	3
1.2.2 A Non-local Hidden Variable Theory	4
1.2.3 Wave function and particles in motion	6
1.2.4 Determinism and Randomness in BM	10
1.3 Particle trajectories in Bohmian Mechanics	13
2 Weak Measurements & Weak Values	15
2.1 Weak Measurement	15
2.2 Pre- and Postselected Systems	20
2.2.1 The Two-State Vector Formalism	20
2.2.2 Measurements on pre- and postselected systems	21
2.3 Weak Value: outcome of weak measurement on PPS systems	22
2.3.1 Definition of Weak Value	22
2.3.2 Unusual properties of Weak Values	23
2.3.3 Experimental realization of weak PPS measurements	24
2.3.4 Applications of Weak Values	24
2.4 Measuring Bohmian trajectories via weak measurement	25
3 The Double-Slit Experiment in the frame of Bohmian Mechanics	27
3.1 Wave-particle dilemma and explanation	27
3.1.1 Standard Quantum Mechanics dilemma	28
3.1.2 Bohmian Mechanics explanation	29
3.2 First observation of average trajectories	33
3.3 Surrealistic trajectories	34
3.3.1 Accusation of surrealism	34
3.3.2 Discussion and state of the art	36
3.4 Mathematical description of the possible scenarios	37
3.4.1 Decoherence	38
3.4.2 Interference	39

3.4.3	Surreal Case	40
3.5	This experiment	41
4	Creation of the setup	43
4.1	General description of the setup	43
4.2	Shaping the Gaussian beam: lenses	44
4.3	Birefringent crystals as double-slit	45
4.3.1	Basic theoretical principles and simulations	45
4.3.2	Experimental realization	46
4.4	Implementation of the Weak Measurement	50
4.4.1	Description of the measurement	50
4.4.2	YVO crystal as entangling medium	53
5	Measurement results	55
5.1	Realistic initial pointer state	55
5.2	Average trajectories of photons	56
	Conclusions	59
	A Definition of the geometrical parameters of the slits	61
	B Discussion of alternative setups	63
	Bibliography	65

Introduction

Many different interpretations of the quantum theory have been proposed since its first conception in the 1920s. Among them, the Copenhagen interpretation [1, 2] has become the most widely recognised. Nevertheless, being affected by some fundamental issues (such as the measurement problem), it is not completely satisfactory. Bohmian Mechanics [3, 4] is a relevant alternative interpretation of the quantum theory. It is a non-local and realistic theory based on hidden variables: the real particles positions. This framework allows conceiving the concept of quantum particle trajectories, which is not permitted in the Copenhagen approach. Still, the two interpretations are totally compatible from an empirical point of view, since they provide exactly the same statistical predictions for the measurement results.

In 1992, the reality of Bohmian trajectories has been questioned by Englert et al. [5] with the proposal of a gedanken experiment. Quantum optics and the theory of weak measurements provide a suitable physical system and the needed operational tools that make the implementation of this gedanken experiment possible [6]. The Bohmian velocity of entangled photons in a double slit apparatus can be weakly measured and thence the Bohmian trajectories reconstructed. In 2016, an experiment was performed which claims to confute the objection raised by Englert [7].

Our planned experiment is a test of the gedanken experiment and a further investigation of Bohmian trajectories in this situation. It is performed under the following conditions (see Fig.1). A pair of path-polarization entangled photons is given: the first photon is sent through a double slit interferometer while on the second one, outside the interferometer, a measurement of polarization is performed. In our experiment those polarization measurements on photon 2 will be performed under conditions which have never been realized before, namely at different moments with respect to photon 1 crossing the interference region and in different polarization bases. How will those different measurement settings influence the trajectories of the photon in the interference region?

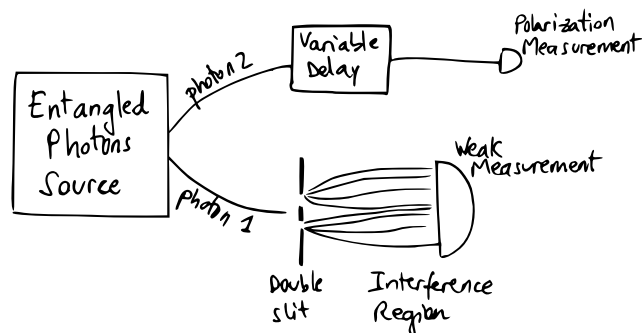


Figure 1: Schematic representation of the experimental setup.

The particular goal of this thesis is firstly setting up the entire branch of the apparatus that concerns the photon whose trajectories are measured. Namely: shaping the beam, creating the double slit using birefringent crystals and implementing the weak measurement of the Bohmian velocity. Secondly, with this setup completed, measuring the Bohmian trajectories in the interference region of the double slit apparatus.

The plan of this thesis is as follows. In the first Chapter an introduction to Bohmian mechanics will be given, with the goal of describing the concept of single particle trajectory; in fact, single photon trajectories will be the object of investigation of the experiment. In the second, the theory of weak measurements will be presented, which provides the possibility for the experimental measurement of the particle trajectories. The double-slit experiment, exemplary demonstration of the explanatory power of Bohmian mechanics, as well as fundamental building-block of our experiment, will be discussed in Chapter 3. The creation of the setup will be described in Chapter 4, while measurement data, analysis and insights will be presented in Chapter 5. Final remarks will be reported in the Conclusions.

Chapter 1

Bohmian Mechanics

At the foundation of Quantum Mechanics (QM), the Copenhagen interpretation established itself despite its manifest unresolved issues. Bohmian Mechanics (BM) manages to get rid of counterintuitive interpretations of quantum phenomena considering QM as a theory describing real particles in motion. Although the two interpretations give the same statistical predictions to experimental results, the ontological basis provided by BM to the quantum theory paves the way for explanations of phenomena that in the orthodox QM are relegated to the realm of impossibility, such as the description of single particle trajectories. Despite its alluring intuitive nature shown in some respects, BM remains a fringe theory. After all, in BM one has to accept a non-local behaviour of the wave function, which causes influences on the particle trajectory in some region of space after some manipulation of the wave function in a well separated other region of space.

1.1 Problems and limitations in orthodox Quantum Mechanics

Still being the most widely accepted understanding of QM, the Copenhagen interpretation is affected by some intrinsic significant problems. Here a couple of them will be presented and others will be encountered in following Sections as further motivations for the proposal of an alternative interpretation of the quantum theory; namely the unnecessary assumptions which induce limitations not inherently required by the quantum theory (Section 1.2.1) and the ambiguous position of the border between what can still be treated as classical and what necessarily requires a new quantum description (Section 1.2.2).

What is Quantum Mechanics about?

Orthodox quantum mechanics is not about what there is. It's just about wave functions and the deriving probabilities of measurement outcomes. It would seem clear that quantum mechanics is fundamentally about atoms and electrons, quarks and strings. But, as an inquisitorial Goldstein asks [8], if these entities are not somehow identified with the wave function itself, then where are they to be found in the quantum description? The wave function is, in fact, not a wave in anything real, but just a mathematical tool that rules the statistics of the experiment results.

In orthodox QM, the statistics of the experiment results is "everything that can be meaningfully said about a physical system" [9]. Even though the possible existence of an objective reality is not denied, it is not the goal of standard QM to provide a description of this reality [9]. According to

Bohm et al. [10], the basically new feature of the quantum theory, on which most interpretations - among which the standard one - agree, is that in this theory “there is no way even to conceive of the individual actual system, except insofar as it manifests itself through the phenomena that are to be observed in such a process of measurement”. The founding fathers of the orthodox QM insisted that in the absence of measurement, an unobserved system is only a suite of possibilities of the various states that the system could take in case a measurement was made. No observables at all are taken seriously as describing objective properties, as actually having values whether or not they are or have been measured. Summarizing, physical systems have no precisely definable reality themselves. To talk about them, one has to rely on measurements and on the statistics of their results.

The measurement problem

Quantum mechanics is all and just about probabilities of measurement results, and still the so-called “measurement problem” is probably the greatest conceptual difficulty that plagues quantum mechanics. The objection known as the “measurement problem” is essentially as follows [8]. Quantum theory provides two rules for the evolution of the wave function of a quantum system: a deterministic dynamics given by Schrödinger’s equation when the system is not being measured or observed, and a random collapse of the wave function to an eigenstate of the measured observable when it is. However, quantum theory does not explain how to reconcile these two apparently incompatible rules. And it is in fact difficult to motivate the idea that different laws than those governing all other interactions should govern those interactions between system and apparatus that we happen to call measurements. Hence the apparent incompatibility of the two rules.

Here is a short analysis of a measurement of a quantum observable assumed to have a non-degenerate spectrum of eigenvalues n and normalized eigenstates $\psi_n(x)$ [11]. Let the initial wave function of the observed system be

$$\psi_0(x) = \sum_n c_n \psi_n(x), \quad (1.1)$$

and $\phi_0(y)$ the one of the measuring apparatus, also denoted as “pointer”. Then the initial wave function of the combined system reads

$$\Psi_0(x, y) = \phi_0(y) \sum_n c_n \psi_n(x). \quad (1.2)$$

After the two system have interacted, by linearity of the unitary evolution, the final wave function Ψ_t of the system and apparatus is itself a superposition:

$$\Psi_t(x, y) = \sum_n c_n \psi_n(x) \phi_n(y), \quad (1.3)$$

where $\phi_n(y)$ are the different wave packets of the relevant parameters of the apparatus that correspond to the possible results of the measurement. Of course, for a proper measurement to be made, the packets $\phi_n(y)$ must be distinct and non-overlapping. This corresponds to the condition for the $\phi_n(y)$ to have disjoint supports in the configuration space of the apparatus:

$$\text{supp}(\phi_i) \cap \text{supp}(\phi_j) = \emptyset, \quad i \neq j. \quad (1.4)$$

However, the fact that the pointer ends up pointing in a definite direction, even a random one, is not discernible in this final wave function. Insofar as orthodox QM is concerned, we have arrived at the measurement problem.

1.2 Introduction to Bohmian Mechanics

Why not just have real waves that push around real particles? This is Bohmian Mechanics, also known as pilot-wave theory. In it, the wave function is the mathematical representation of an objectively real field [3]. This field guides the motion of a real particle that has a definite location at all times. Importantly, the wave function in pilot-wave theory evolves according to the Schrödinger equation. Sharing BM and orthodox QM the fundamental Schrödinger equation, the two theories make exactly the same probabilistic predictions for the measurement results. Despite this essential mathematical consistency, BM distinguishes itself for its fundamental conviction that “it is not necessary to give up a precise, rational and objective description of individual systems at a quantum level of accuracy” [3].

1.2.1 An ontological basis for the Quantum Theory

“As an alternative to the positivist hypothesis of assigning reality only to that which we can now observe, we wish to present here another hypothesis...based on the simple assumption that the world as a whole is objectively real and that, as far as we know, it can correctly be regarded as having a precisely describable and analyzable structure of unlimited complexity”.

D. Bohm, 1952 [4]

When David Bohm first proposed his interpretation of the quantum theory [3], he pointed out that an assumption at the base of the usual interpretation is indeed unnecessary. According to this assumption, the most complete possible specification of an individual system is in terms of a wave function that determines only the probabilities of results of actual measurement processes. Considering this assumption leads to limitations inherent in the conceptual structure of the standard interpretation of QM. Among them, the uncertainty principle and the conviction that a reasonable understanding of the world is impossible.

Bohm strongly criticized this unnecessary restriction required by Copenhagen approach to QM and he showed that, in fact, there is no need to stick to the usual interpretation of QM and to accept the limitations that come along with it, since its fundamental assumption is actually not necessary [3].

The theory that Bohm had in mind was a theory in which objective and precisely definable description of reality is possible also at the quantum level of accuracy. After all, “the problem of objective reality at the quantum level is at least in principle not fundamentally different from that at the classical level” [4].

Thus he suggested a realistic interpretation of the quantum theory in which the wave function is regarded as a real entity and the classical idea of real particles having a definite position at all times is preserved. Taking both wave and particle to be objectively real -whether they are observed or not¹- is the core of the “suggested interpretation of the quantum theory in terms of hidden variables” first proposed by Bohm in 1952 [3, 4]. A more detailed description and development of its ontological basis was later published in the 1980s [10].

So Bohmian Mechanics was conceived: a quantum theory about particles in motion, that spells out what it is about. The new suggested interpretation provides a broader conceptual framework than the usual interpretation, because it makes possible a precise and continuous description of

¹“It seems to be much simpler ... to assume an objective universe, with its particles and with its wave functions, which is not dependent on observers”, Bohm et al. [10].

all processes, even at a quantum level. Thanks to its clear ontology, it leaves therefore no place for paradoxes and release the quantum theory from the forementioned limitations imposed by the orthodox interpretation. Moreover, its broader conceptual framework admits into the theory the existence of entities that cannot be observed yet. This is a good working hypothesis, since, as Bohm himself asserts [3], the purpose of a theory is not only to correlate the results of observations that we already know how to make, but also to suggest the need for new kind of observations and to predict their results. It must be considered that what experimental physics can measure depends not only on the technological development of the available apparatuses, but also on the suggestions and the intuitions provided by the reference theory, which determines the kind of inference that can be used to connect the directly observable state of the apparatus with the state of the system of interest. In other words, our epistemology is determined to a large extent by the existing theory.

1.2.2 A Non-local Hidden Variable Theory

Bohmian mechanics is the most famous and best developed hidden-variable theory for quantum physics. It postulates the existence of both a quantum wave and particles. The exact positions of these particles are the additional “hidden” variables compared to the usual quantum physical description. Note that position is commonly the only property considered as a hidden variable in BM. Other degrees of freedom, such as spin, are regarded as property of the wave function and not of the particle [11, 12].

Statistical physics grounds

The fact that the standard formulation of QM is based on the wave function and on variables adopted from classical physics makes the quantum theory inexact and inaccurate [13]. Those macroscopic classical variables can however be replaced by a quantum analogue of *microscopic* classical variables [14]. In this sense, Bohm’s proposal is to do it like Boltzmann taught us: just as gas molecules move in a box guided in their motion by classical laws, so the N particles of a quantum system are to be regarded as real particles with precisely defined trajectories, guided in their motion by the wave function. Such an approach would lead to a more precise theory; it would be, according to Bell, the way “towards an exact Quantum Mechanics” [15]. In terms of hidden variables and with the words of Bohm himself:

“As a matter of fact, whenever we have previously had recourse to statistical theories, we have always ultimately found that the laws governing the individual members of statistical ensemble could be expressed in terms of just such hidden variables. From the point of view of macroscopic physics, the coordinates and momenta of individual atoms are hidden variables, which in a large scale system manifest themselves only as statistical averages. Perhaps then, our present quantum-mechanical averages are similarly a manifestation of hidden variables, which have not, however, yet been detected directly”.

Bohm, 1952 [3]

Access key to a complete description of quantum phenomena

In order to build confidence in the hidden variable model - showing the great potential that the hidden variable approach could have in a better description of reality -, Bohm proposed an analogy with the early forms of the atomic theory [3]. In that case the existence of atoms was postulated in order to explain certain large-scale effects

that could also be correctly described in terms of existing macrophysical concepts without the requirement of any reference to atoms; ultimately, however, effects were found which contradicted the predictions obtained by extrapolating certain purely macrophysical theories to the domain of the very small, but which could be understood correctly in terms of the assumption that matter is composed by atoms.

Similarly, Bohm suggested that if there are hidden variables underlying the quantum theory, it is quite likely that in the atomic domain they will lead to effects that can also be described adequately in the terms of the usual quantum mechanical concepts; while in a domain associated with much smaller dimensions the hidden variables may lead to completely new effects not consistent with the extrapolation of the present quantum theory down to this level.

These hidden variables could not just allow to go beyond the ranges of applicability of standard QM, but they would also, in principle, “determine the precise results of each individual measurement process². In practice, however, ...the observing apparatus disturbs the observed system in an unpredictable and uncontrollable way, so that the uncertainty principle is obtained as a practical limitation on the possible precision of measurements. This limitation is not, however, inherent in the conceptual structure of [Bohmian] interpretation. ... [In fact,] simultaneous measurements of position and momentum having unlimited precision would be in principle possible” via a suitable mathematical reformulation of the quantum theory which is consistent with Bohmian interpretation but not with the usual one [4].

Non-locality

Pretty soon after de Broglie first proposed pilot-waves, the revered mathematician John von Neumann published a proof showing that hidden variable explanations for the wave function couldn't work. With it he claimed to have proven that Einstein's dream of a deterministic completion of quantum theory was mathematically impossible [16]. That proclamation contributed to the long shelving of pilot-wave theory. Physicists and philosophers of science almost universally accepted von Neumann's claim. For example, Max Born asserted that no hidden parameters can be introduced with the help of which the indeterministic description could be transformed into a deterministic one. Hence if a future theory should be deterministic, it cannot be a modification of the present one but must be essentially different.

But in fact, von Neumann did not develop the argumentation exhaustively: it turned out that the restriction against hidden variables only applies to *local* hidden variables. So there can't be extra information about a specific region of the wave function that the rest of the wave function doesn't know. This was figured out pretty soon after Von Neumann's paper by the German mathematician Grete Hermann. However her refutation wasn't noticed until it was re-derived by John Bell in the 1960s with the article “On the Problem of Hidden Variables in Quantum Mechanics” in which he demonstrates that von Neumann's axioms are unreasonable [12].

With the words of Braveman and Simon [17], “for entangled quantum states, actions performed on one particle can have an instantaneous effect on the motion of another particle far away”. This feature motivated Bell to study the question whether all hidden-variable theories that reproduce the statistical predictions of QM have to be nonlocal. The question was affirmatively answered by Bell's theorem [18], ruling out local hidden-variable models. This helped the revival of Bohmian mechanics, because it doesn't use local hidden variables: its hidden variables are *global*³. The

²see Section 1.2.4 for more details

³The nonlocal character of BM was recognized by Bohm as early as 1952 in [4], where he already showed that

entire wave function knows the location, velocity, and spin of each particle. Not only does the entire wave function know the properties of the particles, but the entire wave function can be affected instantaneously. So a measurement at one point in the wave function will affect its shape elsewhere. This can therefore affect the trajectories and properties of particles carried by that wave, potentially very far away (examples of this interesting behaviour are discussed in Chapter 3).

It should be emphasized that the instantaneous influences experienced by individual Bohmian particles cannot be used for superluminal signaling [17, 10]. The reason for this lies in the fragility of the nonlocal quantum connections. Although the total system is instantaneously interconnected, nevertheless, the actual behaviour of long-range quantum connections is too fragile to be controllable in ways required for transmitting a signal.

1.2.3 Wave function and particles in motion

Bohmian mechanics is a non-relativistic theory describing the behaviour of a system of N point-like particles which move in physical space \mathbb{R}^3 along trajectories.

A complete description of the system, in BM, is not provided by the wave function alone. In this hidden-variable theory, in fact, the state of this system is described by *both* a wave function $\psi = \psi(\mathbf{q}_1, \dots, \mathbf{q}_N) = \psi(q)$, a complex (or spinor-valued⁴) function on the configuration space \mathbb{R}^{3N} of possible configurations q of the system, *and* the actual configuration Q defined by the actual positions $\mathbf{Q}_1, \dots, \mathbf{Q}_N$ of the particles [19, 8].

Wave function and particles are two distinct, coexisting and strictly related entities. In BM, also known as pilot-wave theory, the wave function guides the particle in its motion.

Two defining equations

There are two equations at the basis of BM: one describes the evolution of the wave function, the other the motion of the particle. They are so fundamental that, according to Dürr and Teufel [19], understanding what BM says about the world is just a matter of analysis of those equations.

Schrödinger equation for the wave function

As in standard QM, the wave function

$$\begin{aligned} \psi : \mathbb{R}^{3N} \times \mathbb{R} &\rightarrow \mathbb{C} \\ (\mathbf{q}, t) &\mapsto \psi(\mathbf{q}, t) \end{aligned} \tag{1.5}$$

evolves in time according to the Schrödinger equation:

$$i\hbar \frac{\partial}{\partial t} \psi(\mathbf{q}, t) = \left[-\frac{\hbar^2}{2m} \nabla^2 + V(\mathbf{q}) \right] \psi(\mathbf{q}, t), \tag{1.6}$$

where the operator in square brackets is the Hamiltonian of the system.

With the Schrödinger equation at the basis of both Copenhagen and Bohmian interpretations of QM, the two theories share the same mathematical tools and therefore lead to the same statistical

von Neumann's proof that quantum theory is not consistent with hidden variables does not apply to Bohmian interpretation, because the hidden variables contemplated in the latter depend both on the state of the measurement apparatus and the observed system and therefore go beyond certain von Neumann's assumptions.

⁴Spinor-valued wave functions must be considered in quantum mechanics to describe electrons and other quantum particles that have additional degrees of freedom, such as spin.

prediction of experiments results, i.e. they are empirically equivalent. Though, as Dürr et al. remark [20], BM is the natural embedding of Schrödinger equation when we insist upon the simplest ontology - particles described by their positions - and look for a natural evolution for this ontology.

Guiding equation for the particle

The motion of a particle in physical 3-dimensional space is entirely guided by the wave function. For this reason, Bohmian mechanics is also known as pilot-wave theory. The wave function $\psi(\mathbf{q}, t)$ defines the particle velocity field $\mathbf{v}^\psi(\mathbf{q}, t)$ on configuration space in the following way [19]. Let's recall the quantum flux or probability current \mathbf{j}^ψ , introduced by Madelung early in 1926 [21]:

$$\mathbf{j}^\psi = \frac{\hbar}{2im}(\psi^*\nabla\psi - \psi\nabla\psi^*) = \mu \operatorname{Im}[\psi^*\nabla\psi], \quad (1.7)$$

where μ is an appropriate dimension factor and Im denotes the imaginary part.

Considering

$$\nabla \cdot \mathbf{j}^\psi = \nabla \cdot \frac{\mathbf{j}^\psi}{|\psi|^2} |\psi|^2 =: \nabla \cdot \mathbf{v}^\psi |\psi|^2, \quad (1.8)$$

one obtains the vector field

$$\mathbf{v}^\psi(\mathbf{q}, t) = \frac{\mathbf{j}^\psi(\mathbf{q}, t)}{|\psi(\mathbf{q}, t)|^2} = \mu \operatorname{Im} \left[\frac{\psi^*(\mathbf{q}, t)\nabla\psi(\mathbf{q}, t)}{|\psi(\mathbf{q}, t)|^2} \right], \quad (1.9)$$

which is the field of the Bohmian velocity for the particles in the system.

The integral curves along the vector field (1.9) are seen, in Bohmian mechanics, as the possible particle trajectories. For this reason, (1.9) is a fundamental equation in the pilot-wave theory, known as the “guiding equation”.

In cases in which $\psi(\mathbf{q}, t)$ is a scalar function, namely when it describes particles without spin, the expression for the particle velocity can be reduced to

$$\mathbf{v}^\psi(\mathbf{q}, t) = \mu \operatorname{Im} \left[\frac{\nabla_k \psi(\mathbf{q}, t)}{\psi(\mathbf{q}, t)} \right]. \quad (1.10)$$

Considering an analogy with classical fluid dynamics, it becomes clear why in BM Eq. 1.9 should be regarded as the natural, direct, obvious choice for the velocity [14, 8]. Its definition is in fact the ratio of the quantum probability current \mathbf{j} to the quantum probability density $\rho = |\psi|^2$, just as in classical fluid dynamics \mathbf{j}/ρ is the formula for the velocity of a fluid.

The double interpretation of the wave function

The first step towards an interpretation of the wave function was made by Born who, applying the time-dependent Schrödinger equation to a scattering problem, discovered the powerful empirical meaning of the wave function as a “probability amplitude”. In fact, through its modulo squared $|\psi(\mathbf{q}, t)|^2$, the wave function delivers the theoretical predictions for the probability of finding the particle at position \mathbf{q} at time t .

This intuition was corroborated establishing an identity for any solution of the Schrödinger equation. This identity involves the “probability density” $|\psi(\mathbf{q}, t)|^2$ and has the form of a continuity equation. It is the quantum flux equation

$$\frac{\partial |\psi|^2}{\partial t} + \nabla \cdot \mathbf{j}^\psi = 0, \quad (1.11)$$

where \mathbf{j}^ψ is the probability current introduced in (1.7).

Bohmian mechanics pushes the argument further, managing to give the wave function a second, more fundamental meaning.

As seen above, in BM a vector field for the particle velocity (1.9) is defined. This definition is essentially built on the wave function. Integral curves along this vector field constitute the particle trajectories. Particles moving along these trajectories are thus guided by the wave function, since the vector field is induced entirely by the wave function. In BM then, more than the statistical prediction of measurement results, the prevalent role of the wave function is the definition of the vector field through which the wave function can guide the particle in its motion [3, 10, 19].

The quantum potential

Another interesting derivation of BM can be developed introducing the so-called quantum potential, a mathematical tool which provides a pictorially powerful and intuitive description of the way the wave function fulfils its role of guiding the particle in its motion⁵. The derivation and a discussion of its most relevant features will be presented here. An application of its descriptive power will be presented in Section 3.1.2, in a discussion of the double-slit experiment.

Derivation. Besides the analogy with the classical fluid velocity, there are several other ways to introduce BM [14]. The way Bohm himself adopted [3] was a derivation of his theory through the concept of the quantum potential. With such an approach it would have been easy to capture the intuition of physicist, based on classical physics.

The entire argument is pretty simple and straightforward [8, 22]: write the wave function in the polar form $\psi = R \exp[iS/\hbar]$, where the amplitude R and the phase S are real functions of position and time. Then, the Schrödinger equation reduces to the following two equations:

$$\frac{\partial S}{\partial t} + \frac{(\nabla S)^2}{2m} + V + U = 0 \quad (1.12)$$

and⁶

$$\frac{\partial R^2}{\partial t} + \nabla \cdot \left(R^2 \frac{\nabla S}{m} \right) = 0, \quad (1.13)$$

where V is the classical potential and U is the quantum potential,

$$U = -\frac{\hbar^2}{2m} \frac{\nabla^2 R}{R}. \quad (1.14)$$

Eq. 1.12 is immediately recognized to be the classical one-particle Hamilton-Jacobi equation for S with an additional term: a new quantity, the quantum potential U , appears alongside classical quantities. This feature allows to retain the localized particle with well-defined positions

⁵Note that this can be done without any requirement of additional complexity, since the quantum potential naturally derives from the Schrödinger equation.

⁶For a discussion of Eq. 1.13 as a continuity equation for $\rho = R^2$, with ρ being a probability density, see “The double interpretation of the wave function” in this Section.

and momenta, while the novel aspects of the quantum phenomena can be accounted for in terms of the quantum potential.

It is straightforward that in BM the classical behaviour is clearly approached when the classical potential dominates over the quantum potential. That means that the magnitude of the quantum potential provides a measure of the deviation of Bohmian mechanics from its classical approximation.

Quantum potential as a guiding potential. With the conceptual tool of the quantum potential derived above, it becomes easy to understand how in BM the wave function of an individual particle is regarded as a mathematical representation of an objectively real and precisely definable ψ -field which exerts a force on the particle [3, 4].

In fact, what Bohm did next was using the modified Hamilton-Jacobi equation (1.12) to define particle trajectories just as one does for the classical Hamilton-Jacobi equation, that is, by identifying ∇S with mv , i.e., by setting $\frac{d\mathbf{Q}}{dt} = \frac{\nabla S}{m}$.

This is equivalent to the guiding equation for particles without spin derived above (Eq.1.9). The resulting motion is precisely what would be obtained classically if the particles were acted upon by the force generated by the quantum potential, in addition to the usual forces:

$$F = -\nabla V - \nabla U. \quad (1.15)$$

An interesting analogy with the electromagnetic field is proposed by Bohm in order to make the idea of the ψ -field acting on the particle even clearer: “Just as the electromagnetic field obeys Maxwell’s equations, the ψ -field obeys Schrödinger’s equation. In both cases, a complete specification of the fields at a given instant over every point in space determines the values of the fields for all times. In both cases, once we know the fields functions, we can calculate force on a particle, so that, if we also know the initial position and momentum of the particle, we can calculate its entire trajectory” [3].

New quantum features. Although at first sight it may seem that considering particles acted on by a ψ -field is a return to the older classical ideas, this is indeed not the case: the quantum potential is constitutively provided with novel features which cannot be associated with what is generally accepted as the essential structure of classical physics. An interesting analysis of these quantum features is carried out in [10, 22]. For a deeper understanding of the relation between wave function and particle required in the next chapters, a couple of them will be presented here, as well.

A first property can be seen by noting that the quantum potential (Eq. 1.14) is not changed when the field intensity ψ is multiplied by an arbitrary constant. This means that the effect of the quantum potential depends only on its form and not on its strength, i.e. intensity, as happens with classical waves. This suggests the idea that the ψ -field does not supply energy to the particle, but just guides it: the particle moves under its own energy and the information in the *form* of the quantum wave directs the energy of the particle⁷.

This induces dramatic consequences on the motion of the particle. First of all, it means that particles moving in empty space under the action of no classical forces still need not travel uniformly in straight lines. Moreover, since the effect of the wave does not necessarily fall off with the intensity, even distant features of the environment can profoundly affect the movement,

⁷This feature of the quantum potential explains very clearly the fundamental and specific role performed by the wave function in the Bohmian view of QM, which hence is called “Pilot-Wave Theory”.

thence leading to non-local effects.

A second relevant feature of the quantum potential lies in its dependence on the quantum state of the whole system, in a way that cannot be defined simply as a pre-assigned interaction between all particles. The quantum interconnectedness, acknowledged by Bohm as the most fundamentally new ontological feature implied by the quantum theory [10], has been extensively and accurately described by Philippidis et al. in the work that first presented calculations and pictorial representations of the quantum potential for the realistic situation of the double slit experiment [22]. In their paper it is shown that the quantum potential combines properties of all the participating elements - masses, velocities of particles, widths and separation of slits - in an irreducible way.

1.2.4 Determinism and Randomness in BM

Determinism and randomness coexist in BM. How the conciliation of those opposite concepts can be possible and which implications this fact brings about are the questions addressed in this section.

Determinism

Bohmian mechanics is a realistic quantum theory. It happens to be deterministic, but this is not an ontological necessity. The merit of BM, as stressed by Dürr and Teufel [19], is not determinism, but the refutation of all claims that QM cannot be reconciled with a realistic description of reality. Nonetheless, its determinism makes BM achieve remarkable and interesting results.

Origin of causality in BM. The causal character of the Bohmian interpretation of QM is a direct consequence of the two defining equations discussed in Section 1.2.3 [10, 11]. Since the Schrödinger equation does not involve the particle positions $\mathbf{Q}_i(t)$, it can be solved first and determines the wave functions ψ_t for every time t , once an initial wave function ψ_{t_0} is specified for an initial time t_0 . The wave function ψ_t determines in turn the vector field which always guides the particle,

$$\frac{dQ}{dt} = \mathbf{v}^{\psi_t}(Q(t)). \quad (1.16)$$

Regarding ψ_t as known, this is a time-dependent ordinary differential equation of first order. As such, once the initial configuration $Q(t_0)$ is specified, Eq. 1.16 determines $Q(t)$ for all times. That is why BM is deterministic: once ψ_{t_0} and $Q(t_0)$ are specified, the entire history $Q(t)$ is completely determined by the defining equations (1.6) and (1.9).

The solution to the measurement problem. In Section 1.1 the measurement problem was presented as one of the controversies of Copenhagen approach to QM. Which is now the position of BM concerning this matter? Can Bohmian mechanics reconcile the two dynamical rules for the wave function (the Schrödinger's deterministic evolution and the random collapse)? How does Bohmian mechanics justify the use of the "collapsed" wave function instead of the original one? A positive response was provided in Bohm's first papers on BM ([3], Section 7 and mostly [4], Section 2), where it is said that the suggested interpretation is applied in the theory of the measurement process itself as well as in the description of the observed system. Just as in standard QM, also in BM the act of measurement on a system changes the wave

function. In Bohmian theory, though, this change does not occur through a collapse that is added to the theory, but is rather due to the evolution of the global wave function, describing the interaction of the particle of interest with a measurement device that has its own Bohmian degrees of freedom. What happens in the measurement process can better be regarded as a mutual transformation of observed system and observing apparatus.

Consider the situation described in Section 1.1, the scene left at Eq. 1.3 with orthodox QM stuck in the measurement problem. In this situation BM doesn't run into any problem of this kind, thanks to its realistic approach [10, 11]. As shown by Bohm and Hiley [23], by the time the interaction is over, the "apparatus particles" must have entered one of the wave packets $\phi_n(y)$, say packet m , and will have zero probability of leaving it. The other wave packets (which do not overlap with this one containing the particles) are regarded as "constituting inactive or physically ineffective information" [10]. In BM, in fact, the information enclosed in a wave function becomes active only through a particle that expresses it in its motion. Therefore, these "empty" wave packets carry an information that will always remain just *potentially* active. This information does not contribute to the determination of the quantum potential, which is determined only by the packet $\psi_m(x)\phi_m(y)$. Thus, from now on, all the "empty" wave packets can be ignored [10]. Also at subsequent times, in fact, the development of a significant overlap between the wave packet $\phi_m(y)$ and all the others is prevented by the "effects of decoherence" [8].

Then, in a natural way, without the need for any collapse ever to occur, the state of the system at the end of the interaction is described by the conditional wave function

$$\psi_t(x) = \Psi_t(x, Y_t) = \sum_n c_n \psi_n(x) \phi_n(Y_t) = c_m \psi_m(x) \phi_m(Y_t), \quad (1.17)$$

when the final configuration of the apparatus $Y_t \in \text{supp}(\phi_m)$, i.e. when m is registered.

Randomness

As mentioned, this same deterministic theory gives rise to probabilistic prediction for the measurement results. The grounds of the random character inherent in BM has to be found in statistical physics: as Dürr asserts, "In truth, quantum randomness is good old Boltzmann statistical equilibrium, albeit for a new mechanics" [19].

Intuitive origin of randomness in BM. In principle, the final result of a measurement is determined by the initial form of the wave function of the combined system (particle and measurement apparatus) and by the initial position of the particle and the apparatus variable. In practice, however, we cannot predict or control the initial particle positions with complete precision, hence regarded as hidden variables. Therefore, all that we can predict is that in an ensemble of similar experiments performed under equivalent initial conditions, the probability density is $|\psi|^2$; from this information we are able to calculate only the probability of a given outcome. With this argument Bohm [3, 4] demonstrated that a hidden variables theory, with an underlying deterministic model in which quantum randomness is ascribed to ignorance about the initial configuration of particles in the experiment, is perfectly compatible with the predictions of quantum theory.

An example of this reasoning in a real situation was given in a later article [10], considering the double slit experiment: once the quantum field ψ is specified, the result of each experiment is in principle determinate and depends only on the initial condition of the particle. This initial condition will however fluctuate from one case to the next, because the particle emerges from a

source (e.g., a hot filament) in which they are subject to irregular thermal perturbations. This means that complete predictability and controllability of the initial conditions is, in practice, essentially impossible. In this fashion, statistical notions of the predictions of the quantum theory can be explained while causality is still basic to the theory itself.

Statistical physics grounds of randomness in BM. It can be shown [24] that probabilities for positions given by the quantum equilibrium distribution emerge naturally from an analysis of “equilibrium” for the deterministic dynamical system that BM defines, much as the Maxwellian velocity distribution emerges from an analysis of classical thermodynamic equilibrium. Thus with BM the statistical description in quantum theory indeed takes, as Einstein anticipated, “an approximately analogous position to the statistical mechanics within the framework of classical mechanics”.

Apparent randomness arises because we can’t ever have a perfect measurement of initial position of the particles constituting the system upon which the experiment is performed. Therefore we obtain the “hidden variables” model by regarding the initial configuration of the entire system⁸ as random, with distribution given by the quantum equilibrium hypothesis.

According to this assertion, whenever a system has wave function ψ , then its configuration is random with probability distribution $|\psi|^2$. An important consequence of the quantum equilibrium hypothesis is the empirical equivalence between BM and standard QM.

The consistency of this hypothesis with the time evolution of the system is guaranteed by the notion of equivariance [11, 14]: if the initial configuration $Q(t_0)$ is chosen at random with probability density $|\psi_{t_0}|^2$, then the configuration $Q(t)$ at any other time t is random with probability density $|\psi_t|^2$ (provided the system does not interact with its environment). This fact follows from the continuity equation (Eq. 1.11) for $\rho = |\psi|^2$.

Finally, an important statistical result in the Bohmian approach to randomness is found in the Born rule [25]. To show it, let us consider the situation described for the discussion of the measurement problem. The final state of the system is the conditional wave function $\Psi_t(x, Y_t)$, where the final configuration of the apparatus Y_t is the one corresponding to the outcome m . The probability for this event is, by the quantum equilibrium hypothesis,

$$\int dx \int_{\text{supp}(\phi_m)} dy |\Psi_t(x, y)|^2 = |c_m|^2. \quad (1.18)$$

In the course of the measurement, the wave function of the system is transformed from the initial ψ_0 (Eq. 1.1) to the final ψ_m with probability $|c_m|^2 = |\langle \psi_m | \psi_0 \rangle|^2$. That means that, in BM, the projection postulate arises from the statistical grounds of the theory: in BM Born’s law is not an axiom but a theorem [19].

⁸including the observed system as well as all the measuring instruments and other devices used to perform the experiment.

1.3 Particle trajectories in Bohmian Mechanics

Legitimacy of the notion of quantum trajectories

There is a deeply held conviction, as typified by Zeh [26], that a quantum particle cannot and does not have well defined simultaneous values of position and momentum. As a result of this understanding of the uncertainty principle, the notion of trajectory of an individual particle is strictly inhibited in standard QM. As Hiley and Callaghan remark [27], “actually, the uncertainty principle is not telling us this. What it does say is that we cannot *measure* simultaneously the exact position and momentum of a particle. This fact is not in dispute. But not being able to measure these values simultaneously does not mean that they cannot exist simultaneously for the particle. Equally we cannot be sure that a quantum particle actually does not have simultaneous values of these variables because there is no experimental way to rule out this possibility either. The uncertainty principle only rules out simultaneous measurements. It says nothing about particles having or not having simultaneous x and p . Thus both views are logically possible”. Therefore, if we adopt the assumption that quantum particles do have simultaneous x and p , even though unknown without measurement, we can clearly still maintain the notion of particle trajectory also in quantum processes.

Derivation and properties

As seen in Section 1.2.3, the possible particle trajectories are naturally defined as the integral curves along the vector field $\mathbf{v}^\psi(\mathbf{q}, t)$ (generated by the wave function and defined on configuration space).

It has also been shown that the vector field $\mathbf{v}^\psi(\mathbf{q}, t)$ results from interpreting the squared modulus of the wave function as a probability density, whose transport is given by the quantum flux equation (1.11). Bohmian trajectories are nothing but the flux lines along which the probability gets transported, the streamlines of the probability current. The velocity field is thus simply the tangent vector field of the flux lines.

A noteworthy property of Bohmian trajectories is that they don’t cross each other in configuration space, which makes BM a first order theory [14, 19]. This is an evidence of BM being far from a classical theory, despite the Newtonian appearance of the derivation of the theory via the quantum potential.

Another relevant feature of Bohmian trajectories is their nonlocality. In his a work “On the Problem of Hidden Variables in QM”, Bell points it out as a curious feature of BM: “the trajectory equations for the hidden variables have in general a grossly nonlocal character”. An experimental demonstration of this fact has been given by Mahler et al. in 2016 [7], as proposed by Braveman and Simon [17]. Nonlocality, considered by some the resolution of apparent paradoxes (Hiley et al. [28], Mahler et al. [7]), has been playing an outstanding role in recent discussions about the reality of Bohmian trajectories (see Section 3.3.2).

Meaning

The significance of the one parameter solution of the real part of the Schrödinger equation, namely the modified Hamilton-Jacobi equation of Bohm [4] (Eq.1.12), has been the subject of many discussions over the years. It is important to note that the mathematics is unambiguous and exactly that used in the standard formalism; it is indeed just a matter of interpretation. Attempts to give these solutions physical significance in terms of particle trajectories has often

encountered strong opposition. In fact, some regard them as merely metaphysical baggage with no real physical significance and for this reason their meaning should not be pursued further (Zeh [26], ESSW [5] and Scully [29]). An argumentation that significantly stirred up the discussion is the claim that these “trajectories” lead to results that disagree with the standard interpretation of QM and have such bizarre properties that they should be rather regarded as “surreal”. This objection, raised by Englert, Scully, Süssmann and Walther [5], and the consequent discussion, also supported by experiments, will be presented in more detail in Section 3.3.2.

It is interesting to note [7] that the notion of Bohmian trajectories, although borrowed from the notion of classical particles trajectories, is, in general, different from it. This is because in BM the particles are guided along the trajectories by the wave function. Therefore, only in special situation Bohmian trajectories are Newtonian in character, namely those situations where the guiding wave can be approximated (locally, i.e. there where the particle is) by an almost plane wave. This substantial difference of Bohmian trajectories from classical trajectories enables them to give rise to quantum phenomena, such as the interference produced in a double-slit apparatus.

The concept of Bohmian trajectories is also very different from the Feynman path formalism of quantum mechanics [30]. In the latter, all possible paths between two points are taken into account in the calculation of the transition probability between those two points, while in BM, on the contrary, each particle follows a trajectory in a deterministic manner.

Chapter 2

Weak Measurements & Weak Values

Quantum measurements performed under condition of weak coupling between the observed system and the measurement apparatus are called weak measurements. Due to the weakness of the interaction, measurements of this kind have the particular characteristic of leaving the observed system almost unaltered. Moreover, when applied to a particular type of quantum systems (the so-called pre- and postselected systems), weak measurements yield as outcome the weak value: a physical quantity which provides interesting physical insights in a variety of situations.

The notions of weak measurement and weak value have become important tools for exploring foundational questions in quantum mechanics [31, 32, 33, 34, 35]. In particular, on account of its statistical nature, the weak value offers the possibility to measure average trajectories of single quantum particles.

2.1 Weak Measurement

Quantum Measurement

Quantum measurements are experimentally performed by leading the system under study to interact with the measuring apparatus and measuring the latter afterwards. This process was modelled by von Neumann [16] in the case of projective measurements. His model and its variations [33] are at the base of many studies of quantum measurements.

In von Neumann's measurement model, the measurement device is some external system described by canonical conjugate variables \hat{q} and \hat{p} , with $[\hat{q}, \hat{p}] = i\hbar$. The system-device interaction is designed such that the measurement result is read-off from the effect on some degree of freedom of the measurement device, the so-called "pointer variable", which in the exposition below is taken to be \hat{q} .

A direct extension of the von Neumann measurement model is represented in the following scheme (see Fig.2.1). For a measurement of the system observable \hat{A} at the time $t = t_i$, the quantum system S and the measurement apparatus M, initially in a separable state, get coupled. The coupling interaction is described by the Hamiltonian

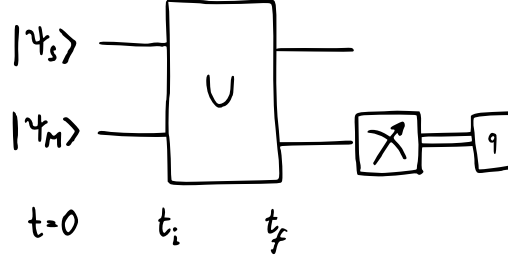


Figure 2.1: Schematic representation of a standard quantum measurement of arbitrary strength. Initially (at time $t = 0$), the system and the measurement device are uncorrelated. Their states are $|\psi_S\rangle$ and $|\psi_M\rangle$, respectively. Through the unitary transformation U in Eq. 2.2, the two systems become entangled. The outcome q of the measurement is read-off by measuring the apparatus pointer variable \hat{q} . Double lines carry classical information.

$$\hat{H} = g(t) \hat{A} \otimes \hat{p}, \quad (2.1)$$

where the normalized coupling function $g(t)$, differing from zero only in the interval (t_i, t_f) , specifies the time of the interaction¹. The action of the measurement process on the two systems is thereby described by the unitary operator

$$U = \exp\left(-\frac{i}{\hbar} \gamma \hat{A} \otimes \hat{p}\right), \quad (2.2)$$

where γ is the coupling strength

$$\gamma = \int_{t_i}^{t_f} g(t) dt. \quad (2.3)$$

The effect of this coupling interaction is a shift δq in the device pointer variable. The amount of this shift is proportional to the expectation value of the observable \hat{A} . The latter can be therefore obtained by simply reading off the final value of the device pointer variable.

This measurement scheme is mathematically presented in the following. The description holds for modelling measurements of arbitrary strength. Afterwards, two kinds of quantum measurements are distinguished, which differ in the regime of the interaction strength: the well-known strong, projective measurement and the novel weak measurement.

Let us assume that the system observable \hat{A} has a set of discrete and nondegenerate eigenvalues $\{a_j\}$ and respective eigenstates $|a_j\rangle$. Expanding the state of the system on the basis of the eigenvectors of \hat{A} , the total initial wave function can be written as

$$|\Psi_I\rangle = |\psi_S\rangle |\psi_M\rangle = \sum_j c_j |a_j\rangle |\psi_M\rangle. \quad (2.4)$$

After the interaction (2.1), the final state reads

$$|\Psi_F\rangle = U |\Psi_I\rangle = \sum_j c_j e^{-\frac{i}{\hbar} \gamma a_j \hat{p}} |a_j\rangle |\psi_M\rangle. \quad (2.5)$$

¹In an ideal quantum measurement the function $g(t)$ is nonzero only during a very short interval of time, during which the free Hamiltonians of the two systems can be neglected.

Introducing the identity operator in position and momentum basis and considering that $\langle q | p \rangle = \frac{1}{\sqrt{2\pi}} e^{\frac{i}{\hbar} p q}$, one obtains

$$\begin{aligned} |\Psi_F\rangle &= \sum_j c_j \iint dq' dp e^{-\frac{i}{\hbar} \gamma a_j p} |p\rangle \langle p | q'\rangle \langle q' | \psi_M\rangle |a_j\rangle \\ &= \frac{1}{\sqrt{2\pi}} \sum_j c_j \iint dq' dp e^{-\frac{i}{\hbar} p(q' + \gamma a_j)} |p\rangle \psi_M(q') |a_j\rangle. \end{aligned} \quad (2.6)$$

Now, a measurement of the apparatus pointer variable q yields

$$\begin{aligned} \langle q | \Psi_F \rangle &= \frac{1}{\sqrt{2\pi}} \sum_j c_j \iint dq' dp e^{-\frac{i}{\hbar} p(q' + \gamma a_j)} \langle q | p \rangle \psi_M(q') |a_j\rangle \\ &= \sum_j c_j \int dq' \underbrace{\frac{1}{2\pi} \int dp e^{-\frac{i}{\hbar} p(q' - (q - \gamma a_j))}}_{\delta(q' - (q - \gamma a_j))} \psi_M(q') |a_j\rangle \\ &= \sum_j c_j \psi_M(q - \gamma a_j) |a_j\rangle, \end{aligned} \quad (2.7)$$

where the integral representation of the Dirac delta function has been used.

That is, the state of the apparatus after the interaction is a mixture of ψ_M located around γa_j and correlated with different eigenstates of \hat{A} .

Strong Measurement

In strong (or projective) measurement, the initial state of the measuring device is such that the value q of the pointer variable is well defined, i.e. its uncertainty $\Delta q = \left(\langle q^2 \rangle - \langle q \rangle^2 \right)^{1/2}$ satisfies the condition

$$\Delta q \ll |\gamma| \min(\delta a), \quad (2.8)$$

with $\min(\delta a)$ being the minimal distance between two consecutive a_j ($\min(\delta a) = \min_j \{a_{j+1} - a_j\}$).

Under this condition, the wavepackets $\psi_M(q - \gamma a_j)$ practically do not overlap. That means that, by reading-off the final value q_f of the device pointer variable, the expectation value of \hat{A} can be determined with very high precision. In fact, for a single event, the final value of q can be uniquely associated with a specific $a_j \gamma$; let us say $a_m \gamma$. Therefore, considering $q_i = 0$ being the initial value of q , the measurement result for the observable \hat{A} would be a_m , proportional to $\gamma a_m = \delta q$.

The effect of a strong measurement is then the collapse of the system to the eigenstate of the measured observable \hat{A} corresponding to the eigenvalues found in the measurement. The projection postulate [25] provides the probabilities $P_j = |\langle a_j | \psi_S \rangle|^2$ for the eigenvalues a_j of \hat{A} . With these probabilities, the average value $\langle \psi_S | \hat{A} | \psi_S \rangle$ for the observable \hat{A} measured on a large ensemble of systems in the state $|\psi_S\rangle$ is

$$\langle \psi_S | \hat{A} | \psi_S \rangle = \sum_j a_j P_j. \quad (2.9)$$

The price to be paid for a high precision knowledge of the observable value is that strong measurements, with the ensuing collapse, disturb the system dramatically, and, with it, the very process under investigation. In some experimental situations, though, a way is needed to reduce this disturbance to an arbitrarily low level. The solution to this problem is found in the “weak” measurement.

Weak Measurement

A weak measurement [33] is a standard measurement described by the Hamiltonian (2.1) with a small interaction strength γ between the system and the measurement apparatus. Since the measurement-induced change of the state is commensurated with the measurement strength [36], the change in the system produced by a weak measurement can be made arbitrarily small.

The weakening of the interaction (2.1) can be achieved by choosing a small coupling strength γ and preparing the measurement apparatus in an initial state such that the uncertainty Δq of the pointer variable q is very large, i.e. creating the measuring condition

$$|\gamma| \max(\delta a) \ll \Delta q, \quad (2.10)$$

where $\max(\delta a)$ is the maximal distance between two consecutive a_j ($\max(\delta a) = \max_j \{a_{j+1} - a_j\}$).

Due to the weakness of the coupling, the pointer variable q of the mixed apparatus function in the final state (2.7) has been only slightly shifted. It is almost independent of a_j , thus the final state is still approximately in the initial separable state. As intended, a smaller disturbance induced by the measurement to the system has been achieved. The price to be paid for this desirable feature, though, is that almost no information about the system is obtained in a single such measurement. As shown in Fig.2.2 (b), in fact, the probability distribution Δq of the pointer variable is still very broad as it was at the beginning (2.10).

The ambiguity of the pointer’s registration can be overcome by repeating the process many times on single members of an ensemble of identically-prepared systems and then averaging the results of the measurements. The measurement error decreases when increasing the size of the ensemble, and thus can be made arbitrarily small (see Fig.2.2, (c): probability distribution of the expectation value of the pointer variable after 5000 weak measurements).

It is interesting to note that, even though the ensemble average for such a procedure is $\langle \psi_S | \hat{A} | \psi_S \rangle$, just as for a strong measurement, the way of extracting the expectation value in weak measurements differs conceptually from that in projective measurements [37, 33]. In fact, whereas in strong measurements $\langle \psi_S | \hat{A} | \psi_S \rangle$ is obtained from the standard definition of the expectation value by the formula (2.9), in the case of weak measurements $\langle \psi_S | \hat{A} | \psi_S \rangle$ is extracted without measuring each P_j individually, but directly from $\langle q_f \rangle - \langle q_i \rangle = \gamma \langle \psi_S | \hat{A} | \psi_S \rangle$, where $\langle q_i \rangle$ and $\langle q_f \rangle$ are the averages of q at $t = 0$ and $t \geq t_f$, respectively.

The weakness requirement of the interaction made in this Section is not an extraordinary one [38]. In fact, many standard experiments performed in the laboratory are indeed weak measurements: all thermodynamical variables are some averages of an extremely large number of microscopical systems. During a typical measurement of a thermodynamical quantity only a negligibly small fraction of the microscopic system is disturbed.

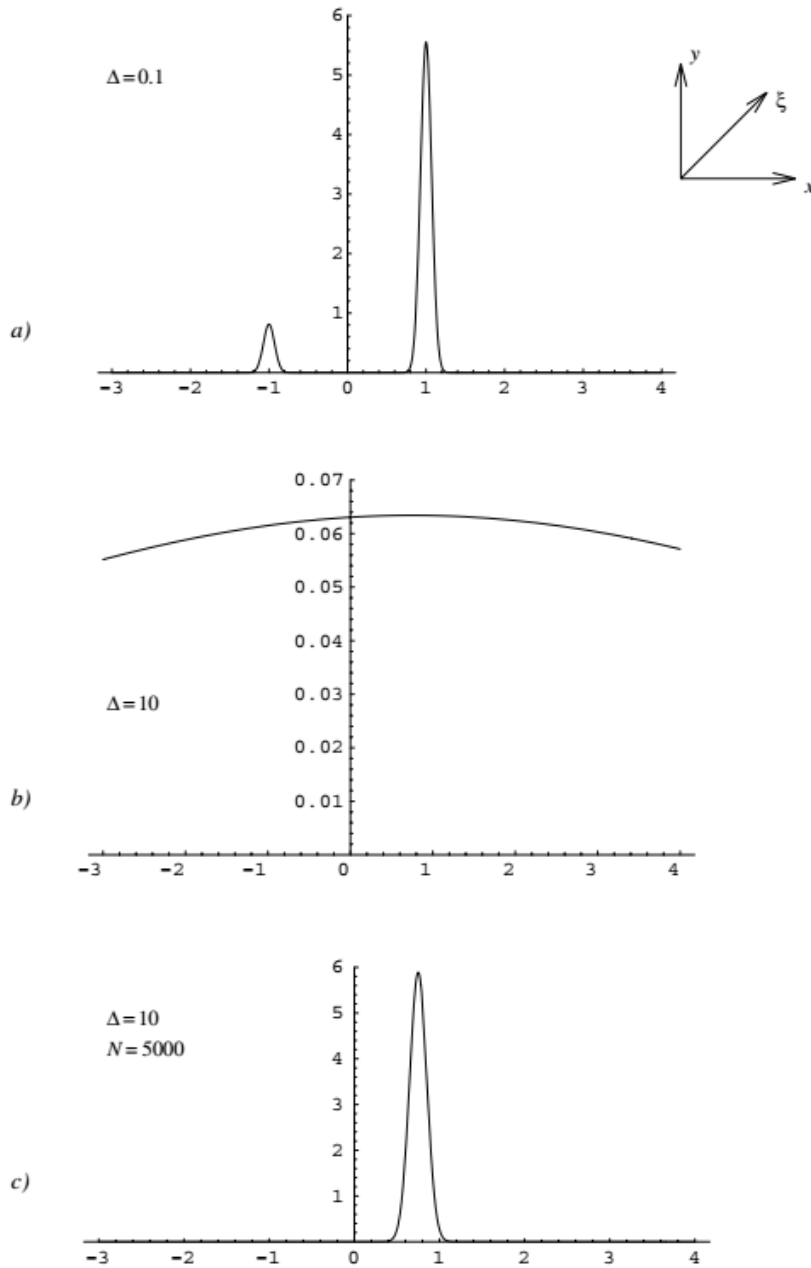


Figure 2.2: Uncertainty of the expectation value of the pointer variable for measurement of spin component in $\hat{\xi}$ direction, i.e. $\sigma_{\xi} = (\sigma_x + \sigma_y)/\sqrt{2}$, on initial state $|\uparrow_x\rangle$. (a) Strong measurement ($\Delta q = 0.1$): the probability distribution of the pointer is localized around the eigenvalues ± 1 of the observable. (b) Weak measurement ($\Delta q = 10$), single shot: the pointer distribution has a large uncertainty. (c) Weak measurement, uncertainty of the expectation value of the pointer variable after averaging over 5000 measurement results: the width of the peak is reduced from $\Delta q = 10$ to $\Delta p = 10/\sqrt{5000} \simeq 0.14$ and the center of the peak is located around the expectation value $\langle \uparrow_x | \sigma_{\xi} | \uparrow_x \rangle = 1/\sqrt{2}$. Image taken from Aharonov and Vaidman [37].

2.2 Pre- and Postselected Systems

2.2.1 The Two-State Vector Formalism

The two-state vector formalism of quantum mechanics is a time-symmetrized approach to standard quantum theory, particularly helpful for the analysis of experiments performed on pre- and post-selected ensembles.

Time-symmetry motivation

In classical mechanics a state of a system at time t is a time-symmetric concept. This is because for a classical system the results of measurements performed on a system in the past uniquely define the results of measurements in the future and vice versa.

In quantum mechanics it is not so: the results of measurements in the past only partially constrain the results of measurements in the future. Hence the fundamental time-asymmetry in the concept of a quantum state [39, 37]. Thus the question arises: does the asymmetry of a quantum state reflect the time asymmetry of quantum mechanics or can this asymmetry be removed by a time-symmetric reformulation of the quantum theory?

Such a time-symmetric formulation is provided by the Two-State Vector Formalism (TSVF), originated from a seminal work of Aharonov, Bergmann and Lebowitz [40] and later reviewed by Aharonov and Vaidman [37].

While in the intrinsically time-symmetric classical mechanics the state of a system at time t can be determined by a complete set of either initial *or* final boundary conditions, in quantum mechanics, for a time symmetric description of a quantum system at time t , complete sets of initial *and* final boundary conditions must be imposed. This description of a quantum state at time t is the two-state vector

$$\langle \Phi | | \Psi \rangle, \quad (2.11)$$

which consists of a quantum state $|\Psi\rangle$ defined by the results of measurements performed on the system in the past relative to the time t and of a backward evolving quantum state $\langle \Phi|$ defined by the results of measurements performed on this system after the time t .

Just as a single quantum state, the two-state vector yields maximal information about the system and describes the same theory with the same predictions as the single quantum state does. The difference is that the standard approach is time asymmetric, since the single quantum state is defined only by results of measurements performed in the past.

Operational definition of a pre- and postselected system

A system described by a two-state vector (2.11) is called “pre- and postselected system” (PPS). In order to have *now*, at time t_{now} , a system which at a previous time t is a PPS system, two measurements have to be done on the system (see Fig.2.3).

A first measurement of an observable \hat{A} at a time $t_1 < t$ will give an outcome a corresponding to the eigenstate $|a\rangle$ of the observable \hat{A} . The state $|a\rangle$ will then evolve between t_1 and t according to the unitary evolution $U(t_1, t) = e^{-\frac{i}{\hbar} \int_{t_1}^t \hat{H} dt}$, governed by the Hamiltonian \hat{H} , to the state $|\Psi\rangle = U(t_1, t) |a\rangle$.

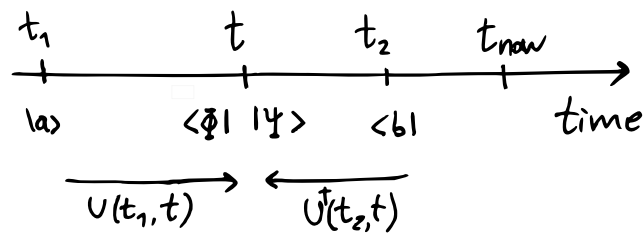


Figure 2.3: Operational definition of a pre- and postselected system.

Equivalently, a second measurement of an observable \hat{B} is performed at a time $t_2 > t$, leaving the system in the state $\langle b|$, which evolves backward in time, from t_2 to t , to the state $\langle \Phi| = \langle b| U^\dagger(t_2, t)$.

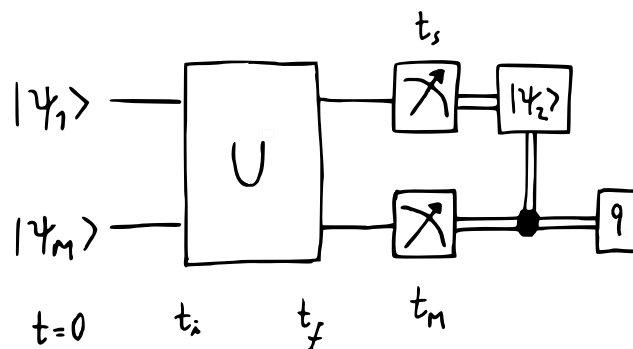
The pre- and postselected system $\langle \Phi| |\Psi \rangle$ is thus experimentally created.

2.2.2 Measurements on pre- and postselected systems

Measurements performed on PPS systems are of particular interest because under certain conditions (see Section 2.3) may yield information on novel quantum properties of the system. Such measurements, which take place in the time interval between the pre- and the postselection of the system, realized on PPS systems are called pre- and postselected (PPS) measurements.

The procedure of the measurement is as follows (Fig.2.3): a large ensemble of particles is prepared at t_1 in the same initial state (preselection). Every particle interacts with a separate measuring device at time t (measurement), and then the measurement which selects the final state is performed at a subsequent time t_2 (postselection).

The measurement scheme introduced in Section 2.1 can be generalized as shown in Fig.2.4 to describe PPS measurements of arbitrary strength [33].

Figure 2.4: Schematic representation of a pre- and postselected measurement. In contrast to Fig.2.1, here the measurement of the pointer variable q is conditioned (“post-selected”) on the measurement of the system S in a state $|\psi_2\rangle$.

Let us consider an ensemble of pairs consisting of a system and a measuring apparatus in the initial pure states² $|\psi_1\rangle$ and $|\psi_M\rangle$, respectively (pre-selection). For each system-apparatus pair the coupling interaction (2.1) is turned on in the interval (t_i, t_f) ; when the interaction is over, the state of each pair system reads

$$|\Psi_F\rangle = U |\psi_1\rangle |\psi_M\rangle. \quad (2.12)$$

Then a PPS ensemble is formed by performing a projective measurement of a variable \hat{B} on each system at $t_S > t_f$ and selecting for further consideration only the systems which collapsed in the eigenstate $|\psi_2\rangle$ of \hat{B} (postselection):

$$\langle\psi_2|\Psi_F\rangle = \langle\psi_2|U|\psi_1\rangle|\psi_M\rangle. \quad (2.13)$$

A PPS measurement is completed by measuring the pointer observable q of the apparatuses at $t_M > t_f$. Note that the changing in time ordering between the pointer observable measurement and the postselection measurement does not affect the results of the statistical analysis of the values of the pointer variable q [38, 33].

A statistical analysis performed on the read-off values will yield the result of the measurement of \hat{A} on the PPS ensemble, e.g. the conditioned average value of \hat{A} or the distribution of the pointer values q . The statistical distribution of the measurement results of \hat{A} for a given postselected subensemble depends on the subensemble chosen and is different from the statistical distribution over the whole ensemble. Thus, the possible results of the measurement of \hat{A} indeed depend on both the initial and the final state of the system.

Note, finally, that the terms “preselection” and “postselection”, despite being very similar, denote conceptually different physical processes: preparation of the initial state and conditioning of the measured statistics on the acquired information, respectively [33].

2.3 Weak Value: outcome of weak measurement on PPS systems

2.3.1 Definition of Weak Value

A weak measurement of \hat{A} performed on an ensemble of systems pre-selected in a state $|\psi_1\rangle$ and postselected in a state $\langle\psi_2|$ yields an outcome called the weak value of \hat{A} [31]:

$$A_w \equiv \frac{\langle\psi_2|\hat{A}|\psi_1\rangle}{\langle\psi_2|\psi_1\rangle}. \quad (2.14)$$

This definition comes as the natural interpretation of the outcome of the measuring device as explained as follows [38, 31, 33]. After the interaction has taken place, each system-apparatus pair of the initial ensemble is in the state

$$|\Psi_F\rangle = e^{-\frac{i}{\hbar}\gamma\hat{A}\otimes\hat{P}}|\psi_1\rangle|\psi_M\rangle. \quad (2.15)$$

²For extension to the cases of arbitrary states ρ and ρ_M see [33].

The subsequent postselection in the state $\langle \psi_2 |$ leaves the system in the measuring device state

$$\begin{aligned} |\psi_M^F\rangle &= N \langle \psi_2 | \Psi_F \rangle = N \langle \psi_2 | e^{-\frac{i}{\hbar} \gamma \hat{A} \otimes \hat{p}} | \psi_1 \rangle | \psi_M \rangle \approx N \langle \psi_2 | \left(1 - \frac{i}{\hbar} \gamma \hat{A} \otimes \hat{p} \right) | \psi_1 \rangle | \psi_M \rangle \\ &= \underbrace{N \langle \psi_2 | \psi_1 \rangle}_{N'} \left(1 - \frac{i}{\hbar} \gamma \frac{\langle \psi_2 | \hat{A} | \psi_1 \rangle}{\langle \psi_2 | \psi_1 \rangle} \hat{p} \right) | \psi_M \rangle \approx N' e^{-\frac{i}{\hbar} \gamma \frac{\langle \psi_2 | \hat{A} | \psi_1 \rangle}{\langle \psi_2 | \psi_1 \rangle} \hat{p}} | \psi_M \rangle, \end{aligned} \quad (2.16)$$

where the approximations hold, up to first order in γ , thanks to the condition of weak measurement.

Comparing this result with Eq.2.5, where the pointer state was the sum $\sum_j c_j e^{-\frac{i}{\hbar} \gamma a_j \hat{p}} | \psi_M \rangle$, one notices that the value $\gamma \frac{\langle \psi_2 | \hat{A} | \psi_1 \rangle}{\langle \psi_2 | \psi_1 \rangle}$ plays indeed the role of the expectation value for the operator \hat{A} in the case of a pre- and postselected state.

A measurement of the pointer variable q on the final state (2.16) yields the real part of the weak value A_w :

$$\langle q \rangle_F = \langle \psi_M^F | \hat{q} | \psi_M^F \rangle = \langle q \rangle_I + \gamma \operatorname{Re}(A_w), \quad (2.17)$$

where $\langle q \rangle_I$ is the initial value of the pointer variable q .

As shown in (2.16), the weak value arises from measurements performed in a linear-response regime. The physical significance of the weak value lies in the fact that in this regime the backaction of measurements on the system is very small, and therefore the weak value provides information on the unperturbed system.

2.3.2 Unusual properties of Weak Values

The weak value has some unusual properties that drastically distinguish it from the expectation value of a variable resulting from a standard measurement.

Complex value. Unlike traditional expectation values of quantum observables, the weak value is, in general, a complex number. In the measurement described above, the imaginary part of the weak value contributes only with a phase to the wave function of the measuring device in the position representation. Therefore, the imaginary part will not affect the probability distribution of the pointer position \hat{q} , which is the information extracted in a usual measurement.

However, also the imaginary part of the weak value has a physical meaning: it affects the distribution of the conjugate variable \hat{p} of the measuring device, namely, it is proportional to the shift δp of the wave function that describes the measuring device in the *momentum* representation³. Thus, measuring the shift of the momentum of the pointer will yield the imaginary part of the weak value [38, 37]:

$$\langle p \rangle_F = \langle p \rangle_I + 2\gamma (\Delta p)^2 \operatorname{Im}(A_w). \quad (2.18)$$

Value outside the range of expectation values. As seen in Section 2.2.2, the result of a PPS measurement depends on the choice not only of the pre-, but also of the post-selection. This turns out to be very interesting in the context of *weak* PPS measurements. Postselection, in fact, makes it possible for weak values to acquire surprising values [38]. For instance, the weak value

³Here the initial value of the pointer variable is considered to be 0, both in p and in q representation. Therefore, the shift of the pointer coincides with its final value $\delta p = p_f$ and $\delta q = q_f$.

of a component of a spin-1/2 particle can be 100 [31]. This happens because the weak value diverges when the overlap $\langle\psi_2|\psi_1\rangle$ tends to zero. Values that lie beyond the spectrum of \hat{A} are also explained in terms of quantum interference of the wave packets onto which the measurement apparatus is expanded after the interaction with the system [41].

As a result of those unusual properties of weak values, the probability distribution $|\psi_M(p)|^2$ of the pointer values corresponding to a weak PPS measurement is in general non-classical [33, 38]. Some weak probabilities may in fact be greater than one or negative or even complex. A mean value - the only meaningful value in the context of weak measurements - calculated over such a non-classical probability distribution, is therefore far from resembling the mean value expected in a traditional situation (2.9).

2.3.3 Experimental realization of weak PPS measurements

Although the procedure to realize weak measurements on PPS ensembles could seem at first quite difficult to perform, it becomes feasible when the measuring device is the observed system itself⁴ [38, 37]. In an experiment designed in this way, after the weak interaction, the information about the measured variable is stored in some other degree of freedom (not the measured one) of the system itself. This other degree of freedom plays therefore the role of the pointer of the measuring device. The advantage of such a design is that the postselection of the desired final state of the particles automatically yields the selection of the corresponding measuring devices. The only requirement for the postselection measurement is that there is no coupling between the variable in which the result of the weak measurement is stored and the postselecting device.

The experiment in which this measurement technique was first suggested is of the standard Stern-Gerlach type, modified to fulfil the requirement of weakness, with both pre- and post-selection included [31]. In it, the weak value of a spin component of a spin 1/2 particle is measured, while the position of the particle itself serves as a pointer of the measuring device. The shift in momentum of a particle, translated into a spatial shift, yields the outcome of the spin measurement. A postselection measurement of a spin component in a certain direction can be implemented by another (now strong) Stern-Gerlach coupling which splits the beam of the particles. The beam corresponding to the desired value of the spin is then analysed to extract the result of the weak measurement.

2.3.4 Applications of Weak Values

“Weak Values offer intuition about a quantum world that is freer than we imagined - a world in which particles travel faster than light, carry unbounded spin, and have negative kinetic energy”.

Aharonov, 2005 [39]

In spite of the enthusiasm manifested by some for the promising power of weak values, their unusual properties raised initially also a certain amount of scepticism [42], supported by the fact that the physical meaning and the significance of weak values have not a straightforward understanding [41, 33]. However, subsequent research has made significant progress in elucidating the interpretation of weak values and indicating a variety of situations where they provide

⁴This knack will be applied also in the experiment presented in this thesis.

interesting physical insights (see [38, 41, 33, 32] and references therein). The fields of physics in which weak values proved to be very useful are various, including fundamentals of quantum mechanics and Bohmian mechanics [6, 43, 44, 34, 45, 35].

2.4 Measuring Bohmian trajectories via weak measurement

An example of the use of weak values to probe foundational questions of quantum mechanics involves Bohmian mechanics. In particular, it has been proven that the Bohmian velocity can be formally expressed as a weak value [6, 43]. With this operational definition, the measurement of Bohmian trajectories has become possible [46, 7].

Bohmian velocity as a weak value

Let's consider the Bohmian definition of particle velocity $\mathbf{v}(\mathbf{q}, t)$ as the standard probability current $\mathbf{j}(\mathbf{q}, t)$ divided by the probability density $|\psi(\mathbf{q}, t)|^2$ (Eq. 1.9). It is interesting to note that, actually, from this definition of velocity infinitely many different dynamics are possible. This arbitrariness is originated by the arbitrariness in the definition of the probability current. In fact, the $\mathbf{j}(\mathbf{q}, t)$ that satisfy the continuity equation (1.11) are in principle infinitely many. Starting from this remark, Wiseman [6] showed that a particular $\mathbf{j}(\mathbf{q}, t)$ can be singled out if one requires $\mathbf{j}(\mathbf{q}, t)$ to be determined experimentally as a weak value. With this work, Wiseman provided an operational definition for the averaged Bohmian velocity, regarding it as a weak value (see also [43]).

To demonstrate how the Bohmian velocity can be viewed as a weak value, let us consider the action of the momentum operator $\hat{\mathbf{p}}$ on the wave function $\psi(\mathbf{q}) = \langle \mathbf{q} | \psi \rangle$ describing a system in q representation:

$$\langle \mathbf{q} | \hat{\mathbf{p}} | \psi \rangle = -i\hbar \frac{\partial}{\partial \mathbf{q}} \psi(\mathbf{q}). \quad (2.19)$$

Rewriting it as

$$\nabla \psi(\mathbf{q}) = \frac{\partial}{\partial \mathbf{q}} \psi(\mathbf{q}) = \langle \mathbf{q} | \frac{i}{\hbar} \hat{\mathbf{p}} | \psi \rangle \quad (2.20)$$

and recalling the definition of Bohmian velocity $\mathbf{v}(\mathbf{q}) = \mu \operatorname{Im} \left[\frac{\nabla \psi}{\psi}(\mathbf{q}) \right]$ (also in Eq. 1.9), the result comes straightforward:

$$\mathbf{v}(\mathbf{q}) = \mu \operatorname{Im} \left[\frac{\langle \mathbf{q} | \frac{i}{\hbar} \hat{\mathbf{p}} | \psi \rangle}{\langle \mathbf{q} | \psi \rangle} \right] = \mu \operatorname{Re} \left[\frac{\langle \mathbf{q} | \frac{1}{\hbar} \hat{\mathbf{p}} | \psi \rangle}{\langle \mathbf{q} | \psi \rangle} \right]. \quad (2.21)$$

That is, the Bohmian velocity is indeed the real part of a weak value. It can be obtained by a measurement of the momentum observable $\hat{\mathbf{p}}$ on a pre-selected ($|\psi\rangle$) and postselected ($|\mathbf{q}\rangle$) ensemble. The position-dependent (Bohmian) velocity information captured in this way makes it possible to reconstruct the Bohmian trajectories.

Measuring average trajectories via weak measurement

In 2011 Kocsis et al. [46] reported the experimental observation of the “average trajectories of single photons” in a two-slit interference experiment. This work caused enormous interest because it seemed to overcome fundamental restrictions of quantum mechanics. Indeed, the simultaneous

strong measurement of the which-path information and the formation of the interference picture are impossible in standard quantum theory (complementarity principle), as well as the simultaneous determination of the coordinates and momentum of the particle with exact precision (uncertainty principle), which makes the measurement of a single particle trajectory impossible. This is because a strong measurement of one quantity destroys the information about its complementary quantity, rendering the successive determination of the latter within a certain limit of accuracy impossible. However, the approach of weak measurements, inducing a negligible perturbation on the investigated system, allows the simultaneous determination of complementary quantities, even though averaged over many events [6, 45].

Chapter 3

The Double-Slit Experiment in the frame of Bohmian Mechanics

The double-slit experiment concerns a phenomenon at the heart of standard quantum mechanics, namely the wave-particle duality. In Bohmian mechanics, the relation between wave and particle is considered in a fundamentally different way: wave and particle are two distinct, real entities which always exist simultaneously. This fact enables Bohmian mechanics to give an interesting explanation of what is observed in a double-slit experiment. Actually, the double-slit experiment is the iconic demonstration of the explanatory power of Bohmian mechanics. Therefore, it is also the typical test-bed for the Bohmian theory itself. Considerable debates on Bohmian mechanics, in fact, take place in a two-slit setup.

3.1 Wave-particle dilemma and explanation

The double-slit experiment setup is briefly described in the following. Let us consider to perform the experiment with electrons¹. A source successively emits single electrons, with a fairly large angular distribution, towards an impenetrable wall. The wall has two holes, big enough to let the electron pass through. Beyond this wall there is a screen. Electrons that are not stopped by the wall pass through the holes and reach the screen. The number of electrons hitting the screen at a certain position is measured by detectors placed at different positions of the screen.

The distribution of the electrons at the screen cannot be explained with the laws of classical physics. In fact, it is not the trivial sum of the distributions obtained in the cases of each hole opened alone. The distribution of the electrons shows interference, as if the experiment was done with water-waves [48] (see Fig. 3.1).

Evidently, this experiment requires quantum principles (for this reason it is an emblematic experiment of quantum mechanics). Standard quantum mechanics and Bohmian mechanics have two different approaches for the description of this experiment.

In standard QM the description of the two-slit experiment is given by means of the concept of wave-particle duality. In this framework, trajectories of the particles cannot even be conceived whenever the interference pattern is observed.

¹The experiment can be realized even with semi-macroscopic objects, e.g. fullerene molecules (Zeilinger et al. [47]).

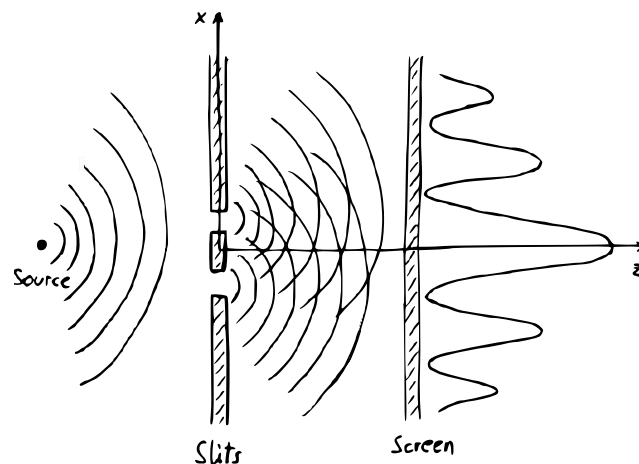


Figure 3.1: Schematic representation of a double slit apparatus. The distribution of the electrons on the screen shows an interference pattern.

In Bohmian mechanics, in contrast, the coexistence of wave and particle enables the description of the interference pattern with a simultaneous definition of the particle trajectory.

3.1.1 Standard Quantum Mechanics dilemma

“[The two-slit experiment shows] a phenomenon which is impossible, *absolutely* impossible, to explain in any classical way, and which has in it the heart of quantum mechanics. In reality, it contains the *only* mystery. We cannot make the mystery go away by ‘explaining’ how it works. We will just *tell* you how it works”.

Feynman, 1964 [48]

As mentioned above, the result of the experiment is the formation of an interference pattern, a typical wave behaviour. Therefore, in the usual quantum interpretation of the experiment, the electron is considered as a wave (described by the wave function $\psi(\mathbf{x})$). The initial plane wave sent towards the wall is modified by diffraction and interference effects when the wave passes through the two slits. Consequently, the single-electron wave will develop a characteristic intensity pattern by the time it reaches the screen. The single electron will be then detected on the screen between position \mathbf{x} and $\mathbf{x} + d\mathbf{x}$ with probability $|\psi(\mathbf{x})|^2 d\mathbf{x}$. If the experiment is repeated many times under equivalent initial conditions, the mentioned interference pattern is eventually obtained.

In standard quantum theory, the origin of this interference pattern contradicts classical intuition, at least in the following ways [3].

Firstly, there may be certain points on the screen where the wave function is zero when both slits are open, but not zero when only one slit is open. How can the opening of a second slit prevent the electron from reaching certain points that it can reach when this slit is closed?

Secondly, even though the wave aspect of the electron must have something to do with the production of the interference pattern, it seems problematic to identify the electron with the wave, since the latter spreads out over a wide region whereas, at the detector, the electron always appears as if it were a localized particle.

The complementarity principle

To deal with this wave-particle behaviour, the standard quantum theory provides two complementary models, the wave-like and the particle-like model. Conditions under which a model is made more precise necessitate a reciprocal decrease in the degree of precision of the other [3]. This solution, known as the complementarity principle, indeed leaves open the dilemma of the appearance of both particle and wave properties of a quantum object in one same phenomenon. According to this principle, if we wish to obtain an interference pattern (wave-picture), the position of the electron (particle-picture) must be unknown; in particular, it is not possible to know through which slit the electron actually passed.

In fact, if an actual experiment is performed to try to get such information, say by placing a measuring device behind one of the slits, the outcome of the original experiment changes: the fringes are no longer produced. It is therefore not possible to design an experiment to track the particle position while retaining the interference pattern. As a result, it is argued that the question as to which slit the electron passed through should not even be raised.

It is then clear that, if the concept of trajectory was meaningful in the standard quantum theory, it would be anyway inconceivable in a double-slit experiment in presence of interference.

3.1.2 Bohmian Mechanics explanation

In Bohmian mechanics, wave and particle exist simultaneously and they behave as expected for an object of their kind (in Feynman's analogy [48], as a water-wave and a bullet, respectively). Accordingly, in a double slit experiment, the wave passes through both slits, whereas the particle passes either through one or through the other slit [11, 19].

The motion of the particle in the interference region is guided by the wave function. As seen in Section 1.2.3, this dynamics is easily describable through the quantum potential. Due to the quantum interconnectedness, changes in the setup induce changes in the shape of the quantum potential, altering eventually the motion of the particle. Thanks to the quantum potential, in this Bohmian scenario the double-slit experiment is described "in terms of a single precisely definable conceptual model" [3].

The quantum potential

The wave function considered here ($\psi = R \exp[iS/\hbar]$) is the same as the one used in the standard description. But now it is regarded as a mathematical representation of an objectively real field that determines part of the force acting on the particle.

The particle is at all times acted on by the quantum potential (Eq. 1.14),

$$U = -\frac{\hbar^2}{2m} \frac{\nabla^2 R}{R}.$$

While the particle is travelling towards the double-slit, this potential vanishes because the wave amplitude R is a constant there; but after passing through the slits, the particle encounters a quantum potential that changes rapidly with position. The subsequent motion of the particle may therefore become quite complicated. This potential, first calculated by Philippidis et al. [22], is shown in Fig. 3.2, as viewed from the screen looking towards the slits. The position of the slits coincides with the two small and symmetric peaks in the background.

Through the quantum potential approach, it is explained why particles are not to be found at points of destructive interference, i.e. at points where the wave function vanishes ($R \rightarrow 0$). The reason is that the quantum potential, U , becomes infinite when R becomes zero. If the approach

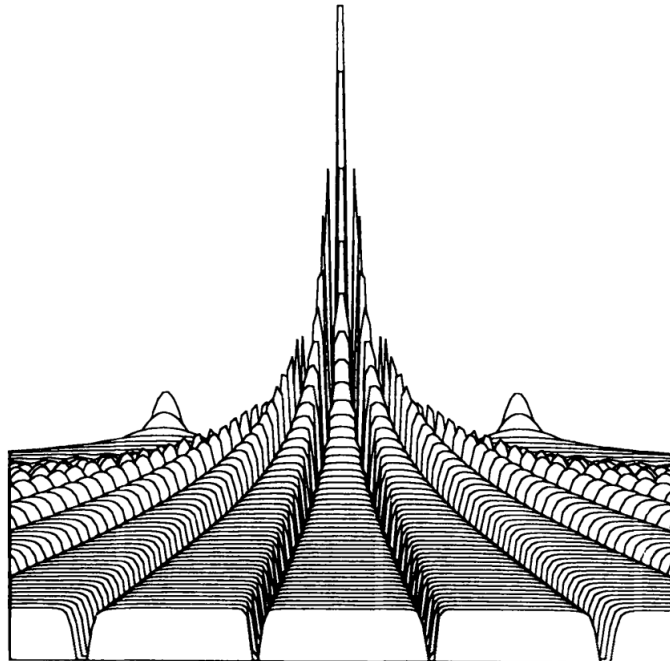


Figure 3.2: Quantum potential of a double slit apparatus, viewed from the screen. First theoretical calculation, by Philippidis et al. [22].

to infinity happens to be through positive values of U , there will be an infinite force repelling the particle away from such a point. If the approach is through negative values of U , the particle will go through this point with infinite speed, and thus spend no time there [3]. In either case, the quantum potential justifies the absence of particles at the points of destructive interference of the guiding wave, explaining in this way the interference pattern of the particle distribution.

Particle trajectories and interference

Following the shape of the quantum potential, particles travel from the slits to the screen. Their trajectories are depicted in Fig.3.4 for various initial positions within each of the two slits. Philippidis et al. [22] calculated those trajectories by integrating the equation

$$v(\mathbf{q}, t) = \frac{1}{m} \nabla S(\mathbf{q}, t), \quad (3.1)$$

which relates S , the real phase of the wave function ψ , to the particle velocity v .

A clear comment on those trajectories made by the same authors is reported here. “Initially the trajectories from each slit fan out in a manner that is consistent with diffraction at a single slit. The subsequent kinks in the trajectories coincide with the troughs in the quantum potential. They arise because, when a particle enters the region of a trough, it experiences a strong force in the x direction which accelerates the particle rapidly through the trough into a plateau region where the forces are again weak. In consequence, most of the trajectories run

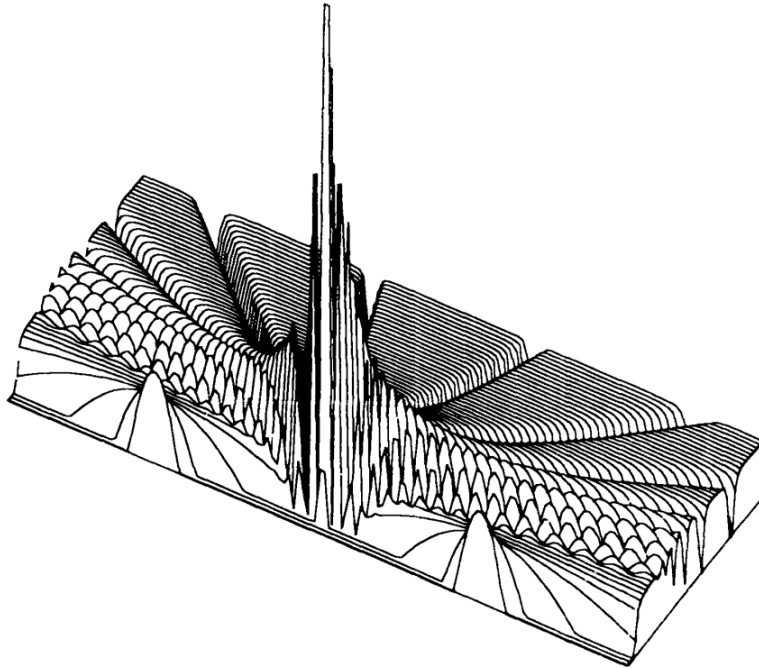


Figure 3.3: Quantum potential of a double slit apparatus, 150° azimuthal view. First theoretical calculation, by Philippidis et al. [22].

along the plateau regions, giving rise to the bright fringes, while the troughs coincide with the dark fringes”.

The fact that trajectories cross the troughs allows them to gather around the $x = 0$ axis, which is the region of the main maximum, the most clearly visible on the screen.

As can be seen in Fig.3.3, “immediately behind the slits the cross section of the initial parabolic peaks first increases slowly, causing the trajectories to spread out radially. This feature corresponds to the spread of the wave packet in the usual approach” [22]. Moving away from the slits towards the screen, high, rapidly varying spikes appear and finally decay into the background. Very few electrons actually reach this region, which can be therefore regarded as lying in the geometric shadow of the two slits (See Fig.3.4).

Those 2D Bohmian trajectories are also characterized by a symmetrical behaviour which will play a relevant role in a following discussion (see Section 3.3) [5]. As one can see in Fig.3.4, the trajectories do not cross the $x = 0$ axis, and are, in fact, symmetric with respect to it. In the interference region between the slit plane and the screen, the wave function is the coherent superposition of the two contributions from the slits,

$$\psi(x, z, t) = \psi_>(x, z, t) + \psi_<(x, z, t). \quad (3.2)$$

Because of the geometrical symmetry of the slits, $\psi_<$ is obtained from $\psi_>$ by reflection at the $x = 0$ axis:

$$\psi_<(x, z, t) = \psi_>(-x, z, t). \quad (3.3)$$

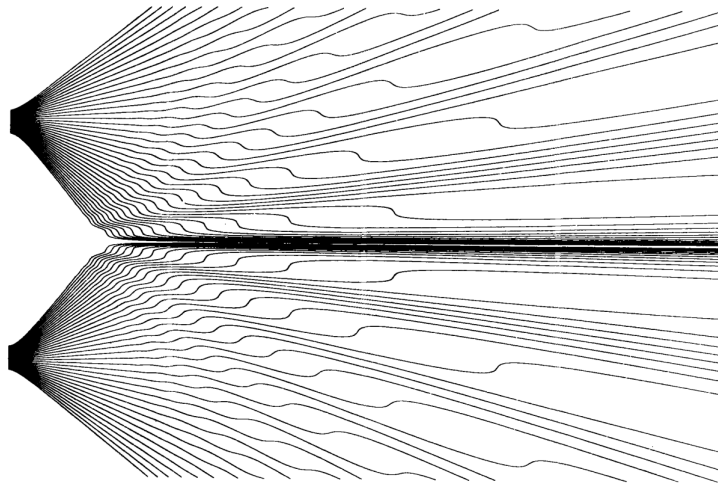


Figure 3.4: Particle trajectories in the interference region of a double slit apparatus. First theoretical calculation, by Philippidis et al. [22].

Consequently, the probability density $\rho = |\psi|^2$ and the x component of the current vector \mathbf{j} (Eq.1.7) are even functions of x , while the x component of \mathbf{j} is odd. Therefore, the x component of the velocity field $\mathbf{v} = \mathbf{j}/\rho$ (Eq.1.9) is also an odd function of x . As a result, the x component of the velocity vanishes on the $x = 0$ axis of symmetry.

This fact has the immediate implication that the Bohmian trajectories do not cross the $x = 0$ axis. A straightforward consequence of this argument is that if a particle hits the upper half of the screen (where $x > 0$), it must have come from the upper slit (the one lying at $x > 0$ position), while a particle arriving on the lower half of the screen (where $x < 0$) has passed, according to Bohmian mechanics, through the lower slit. That means, that the final position of the particle on the screen allows us to deduce through which slit the particle actually passed.

The approach through the quantum potential retains the concept of a point-like particle which follows a well defined trajectory (passing through one or the other slit), while, at the same time, an ensemble of such particles produces the observed interference pattern. This approach removes therefore the ambiguity of whether quantum objects are waves or particles and provides, instead, a clear intuitive understanding of quantum interference in terms of well-defined particle trajectories.

In Bohmian mechanics, the interference (wave-like) pattern can be explained in terms of particles thanks to the quantum equilibrium hypothesis (see Section 1.2.4). According to this hypothesis, in an ensemble of identical particles each having wave function ψ , the empirical distribution of positions is $|\psi|^2$ -distributed [19]. In the double-slit experiment, the random arrival positions of the single particles on the screen will eventually form a recognizable interference pattern, which is essentially the quantum equilibrium $|\psi|^2$ distribution. This distribution is, in fact, the quantum flux across the surface of the screen integrated over time.

The randomness of the arrival position on the screen (like the randomness of the choice of the slit through which the particle passes) is due to the randomness in the initial position of the particle with respect to the initial wave packet emitted by the source. By always preparing the same initial wave packet ψ , the ensemble of $|\psi|^2$ -distributed position is prepared.

Non-locality

An important feature of the quantum potential is non-locality, by Philippidis et al. also efficaciously called “quantum interconnectedness”. Interesting effects of this characteristic are manifest in the double-slit experiment and its variations. As shown in [22], the quantum potential combines properties of all the participating elements - masses, velocities of particles, widths and separation of slits - in an irreducible way. This suggests that, as far as the quantum domain is concerned, space appears to be structured in a way that exerts constraints on whatever processes are embedded within it - e.g., particles travelling towards the screen.

This structure arises out of the properties of both the particle and the apparatus. Therefore, a change in the experimental conditions induces a change in this structure. This eventually results in a modification of the motion of the particle (see Section 3.4 for a description of three different cases).

For example, if one of the slits is closed, the quantum potential is correspondingly altered. Guided by the new structure, the particle may be then able to reach certain points which it was unable to reach when both slits were open.

As another example, let us consider now to place a measuring device at the position of the slits, to detect through which slit the electron passes (the same argument is valid also when the device is placed in any other position of the interference region). The measuring apparatus will alter the quantum potential, creating a disturbance that destroys the interference pattern.

Note that in the last example the result is, of course, the same as in the standard interpretation. However, as Bohm highlighted in 1952 [3], in Bohmian mechanics “the necessity for this destruction is not inherent in the conceptual structure; the destruction of the interference pattern could in principle be avoided by means of other ways of making measurements, ways which are conceivable but not now actually possible”. This is indeed a very interesting remark, which finds in the weak measurement technique an experimental realization (see Sections 3.2 and 4.4).

3.2 First observation of average trajectories

In 2011, Kocsis et al. [46] demonstrated experimentally that particle trajectories in the double slit experiment can be reconstructed for an ensemble of particles with a simultaneous observation of the interference pattern. This has been possible thanks to the weak measurement technique (see Chapter 2). In fact, as explained in Section 2.4, weak measurements provide an operational definition of particles Bohmian velocity, which enables the measurement of average quantum trajectories. In the experiment of Kocsis et al., single photons emitted by a quantum dot are sent through a double-slit interferometer. In the interference region, a weak measurement of the photon momentum is performed by using a calcite crystal that couples the momentum of the photons to their polarization (the pointer variable). The photon polarization is then measured, allowing the weak value of the momentum to be extracted. A final strong measurement of the photon position in a series of planes implements the postselection. The reconstructed average trajectories, reported in Fig.3.5, are indeed congruent with the theoretical trajectories of [22] shown in Fig.3.4.

An interesting classical interpretation of these trajectories was given by Bliokh et al. [44]. They viewed the average over many events, required by the weak measurement method, as a multi-photon limit of classical linear optics².

²All the measurements presented in this thesis, included the average trajectories of photons are performed in a classical optics regime.

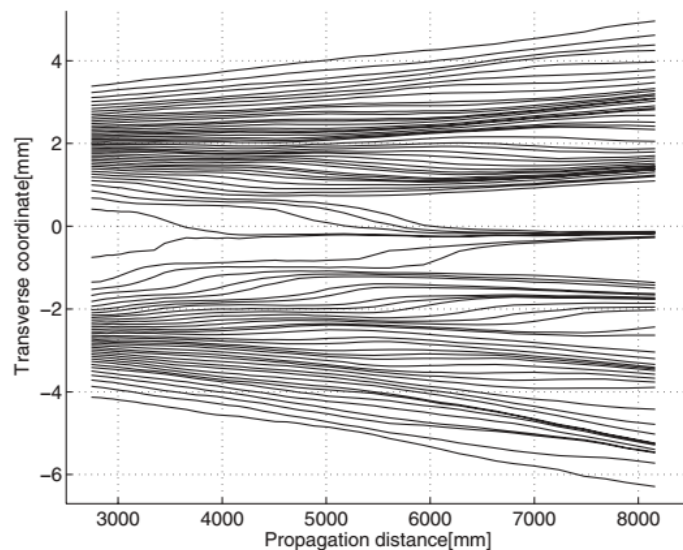


Figure 3.5: Average trajectories of single photons observed in the interference region of a double slit apparatus. First experimental reconstruction, by Kocsis et al. [46].

3.3 Surrealistic trajectories

In 1992, a setup analogous to a double-slit apparatus was chosen as setting for an experimentum crucis. This experiment had the intent to show that “the trajectories, which David Bohm invented in his attempt at a *realistic* interpretation of quantum mechanics, are in fact *surrealistic*” [5]. This interesting and provocative publication gave rise to an intense debate supported by theoretical and experimental argumentations.

3.3.1 Accusation of surrealism

Englert, Scully, Süssmann and Walther (ESSW) based their accusation of surrealism on the following argument [5]. Let us consider a double-slit apparatus. As explained in the previous Section, because of the symmetry of the two wave functions originating at the slits (3.3), in BM one can say through which slit the particle has passed just by looking at the arrival position of the particle on the screen (Bohmian *retrodicted* trajectory). If the particle hits the screen in the upper half, it must have passed through the upper slit; if it arrives at the lower half, it must have passed through the lower slit.

ESSW begin their argumentation remarking that $|\psi_{>}|^2$ does not vanish in the lower half of the screen, which means that the probability for the particle to pass through the upper slit and end up at the lower part of the screen is not zero.

In the ideal experiment that ESSW propose, one-bit which-way detectors are placed in the setup to record through which slit the particle goes. The detectors are such that they not disturb the motion of the particle center of mass. They are also thought to store the which-way information until the particle has reached the screen; afterwards the information is read off. This information enables to clearly distinguish one class of tracks from another, macroscopically different one, namely the class of tracks through one slit from the class of tracks through the

other slit. Having this information implies, of course, the loss of the interference pattern but this is not the issue here. What matters here is that it turns out that the track recorded by the which-way detectors may be macroscopically at variance with the Bohmian retrodicted trajectory. Hence, the surreal nature of Bohmian trajectories.

In particular, this is always the case when the experiment is performed with magnetic atoms traversing an incomplete Stern-Gerlach interferometer. This setup is equivalent to the double-slit interferometer as far as symmetry is concerned, therefore the retrodiction argument of the Bohmian interpretation still holds.

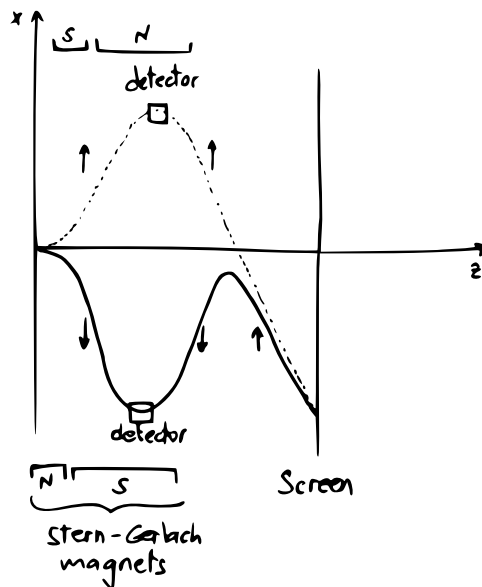


Figure 3.6: Incomplete Stern-Gerlach interferometer with one-bit which-way detectors. For a particle arriving in the lower half of the screen, two conflicting trajectories are drawn: the dashed curve represents the particle trajectory argued in [5]; the solid curve reproduces the Bohmian retrodicted trajectory. The arrows indicate the particle spin.

In Fig.3.6 a schematic representation of the gedanken experiment proposed by ESSW is shown. The event of a particle hitting the lower half of the screen is considered. The macroscopically different behaviour of the recorded track and the Bohmian trajectory is shown.

The dashed curve represents the particle trajectory argued in [5]: due to the geometry of the magnets, when a spin up (\uparrow in the figure) enters the interferometer, it is recorded by the upper detector and hits the screen in the lower half.

The solid curve, on the other hand, represents the Bohmian trajectory of a particle arriving at the lower half of the screen. As a typical Bohm trajectory, it doesn't cross the $x = 0$ axis. Therefore the particle must have gone through the lower detector. By doing so, though, a spin-flip must happen instantaneously at the moment in which the Bohmian particle starts travel away from the $x = 0$ axis (\downarrow turns into \uparrow in the figure).

For ESSW then, at least two valid reasons are there that show the surreal nature of the Bohmian trajectories: (i) the particle goes through a detector, but leaves its mark in the other one; (ii) an unexplained, instantaneous spin-flip occurs.

3.3.2 Discussion and state of the art

The accusation of surrealism provoked a huge discussion in the scientific community of Bohmians (for a brief review see [29]). Various argumentations were presented to defend the *real* status of the Bohmian trajectories. Among them, the self-destructive logic of ESSW [20] and the incorrect usage of the theoretical framework (a comparison between Bohmian trajectories and a standard QM behaviour of the particle is not meaningful, since in orthodox QM the concept of particles travelling along paths doesn't exist) [20, 27, 49].

A crucial argument against ESSW was presented already in 1993 by Dewdney et al. [49] and reconsidered in 2000 by Hiley et al. [28]. It is based on the non-local character of Bohmian mechanics. According to it, the experimentum crucis of ESSW does not reveal anything surrealistic about Bohmian trajectories, but rather shows a manifestation of the nonlocal quantum potential. A which-way detector in an interferometer does not behave in the same way as an isolated detector. It acts under the effect of the non-local quantum potential. This means that the detector can change state, firing, also when the particle travels along the other arm of the interferometer. Therefore, the information read off from such a “fooled” detector can not be trusted.

Regarding the spin-flip issue, as already ESSW had imagined, the problem is not present in Bohmian mechanics, since the spin is not a property carried by the particle itself, but rather a property of the wave function.

Even though repudiated by Hiley himself some years later [27], the argument of non-locality offered the inspiration for a (claimed) experimental validation of the real nature of Bohmian trajectories [7]. The goal of that experiment is twofold.

Firstly, the authors provide an empirical demonstration the non-locality of Bohmian trajectories. This demonstration was performed using a pair of entangled photons, as proposed by Braveman et al. in [17]. From the Bohmian perspective, in fact, the entanglement between the two photons, making their evolution inseparable even when they are spatially separated, accounts for non-locality. The dependence of the trajectory of the first photon on the position of the second photon demonstrated the Bohmian concept of non-locality.

Secondly, the surreal issue was addressed. To reproduce the ESSW measurement scenario, entanglement is necessary. This inevitably leads to non-local effects, as discussed above. In their setup, the condition leading to “surreal” trajectories of the first photon was realized when using the second photon to probe the position of the first. Specifically, the which-way information was encoded in the polarization degree of freedom of the second photon. With this setup the gedanken experiment conceived by ESSW was realized. Mahler et al. [7] indeed observed Bohmian trajectories originating at the lower slit (which should correspond to vertical polarization of photon 2) accompanied by which-way measurement results associated with the upper slit (photon 2 horizontally polarized). A deeper analysis of the origin of this effect, though, reveals that nothing surreal is going on, from the Bohmian perspective. The spin of photon 2, in fact, is not a reliable observable to look at in order to know whether photon 1 passed through the upper or the lower slit. It is not reliable because it is not a constant of motion, but rather evolves in time with the evolution in position of photon 1, to which it is entangled (see Fig.3.7). Therefore the information “stored” in the which-way measurement device is in turn not reliable. Showing that the which-way measurement device is not trustworthy, the ESSW argumentation falls down.

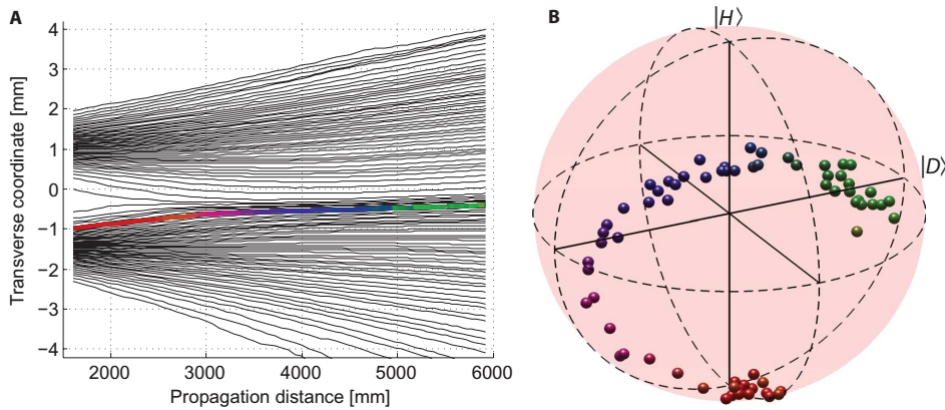


Figure 3.7: Observation of “surrealistic” trajectories. The effect of the nonlocal coupling between the motion of photon 1 and the polarization of photon 2 is shown: as the position of photon 1 evolves in time (A), it causes a change of the polarization of photon 2 over time (B). Therefore, the final polarization state of photon 2 does not provide the correct which-way information of photon 1. Image taken from [7].

3.4 Mathematical description of the possible scenarios

In this Section three relevant configurations of the double-slit apparatus are mathematically described. The first two are the cases traditionally considered, namely (i) the configuration with only one slit open (decoherence) and (ii) the configuration with both slits open (interference). The third case presented is the configuration conceived by ESSW to show the “surrealistic” trajectories.

To illustrate them in a concrete situation, let us consider a quantum optics setting. Pairs of entangled photons are emitted by a source. The wave function of the single pair is

$$|\Psi\rangle \neq |\psi_1\rangle \otimes |\psi_2\rangle. \quad (3.4)$$

In all the three cases, the first photon of the pair is sent towards a double-slit apparatus. The second, on the other hand, is measured each time in different ways. Each measurement condition will affect the distribution of photons 1 on the screen in a different manner.

The entanglement between the photons is initially in the polarization degree of freedom:

$$|\Psi\rangle = \frac{1}{\sqrt{2}}(|H\rangle|H\rangle + |V\rangle|V\rangle). \quad (3.5)$$

The polarization information they carry can be converted into path information via optical components. For this purpose, a beam displacer and a polarizing beam splitter (PBS) are used for photon 1 and photon 2, respectively. Specifically, the beam displacer acts itself as double-slit³, associating horizontal polarization (H) to slit A and vertical polarization (V) to slit B. Similarly, the PBS selects a path for the second photon, according to its polarization. Polarization will be therefore used as label for the path: $|\psi_H\rangle$ and $|\psi_V\rangle$ are the two possible wave functions for

³For more details see Section 4.3.

photon 2 at the exit of the PBS. They are assumed to have completely disjoint support in real space, so that

$$\psi_H(\mathbf{q}_2) \cdot \psi_V(\mathbf{q}_2) = 0 \quad (3.6)$$

holds for all possible position \mathbf{q}_2 of photon 2.

In all the cases, the Bohmian velocity $\mathbf{v}_1(\mathbf{q}_1, \mathbf{q}_2)$ of photon 1 in the interference region will be shown (Eq.1.9); when possible, in the reduced form (1.10).

3.4.1 Decoherence

In this first case, photon 2 is sent through the PBS before photon 1 reaches the double slit (see Fig.3.8). Exiting the PBS, photon 2 will make one of the two detectors fire, revealing its polarization. This accounts as a strong which way detection, which destroys the interference pattern. In fact, due to the entanglement of the two photons in the polarization degree of freedom (Eq.3.5), a measurement of the polarization of the first photon collapses the second in the same eigenstate of polarization.

Once the polarization entanglement has been translated into path entanglement, the total wave function reads

$$|\Psi\rangle = \frac{1}{\sqrt{2}}(|\psi_A\rangle|\psi_H\rangle + |\psi_B\rangle|\psi_V\rangle). \quad (3.7)$$

In real space, as preferable in BM, the total wave function can be written as

$$\Psi(\mathbf{q}_1, \mathbf{q}_2) = \frac{1}{\sqrt{2}}(\psi_A(\mathbf{q}_1)\psi_H(\mathbf{q}_2) + \psi_B(\mathbf{q}_1)\psi_V(\mathbf{q}_2)). \quad (3.8)$$

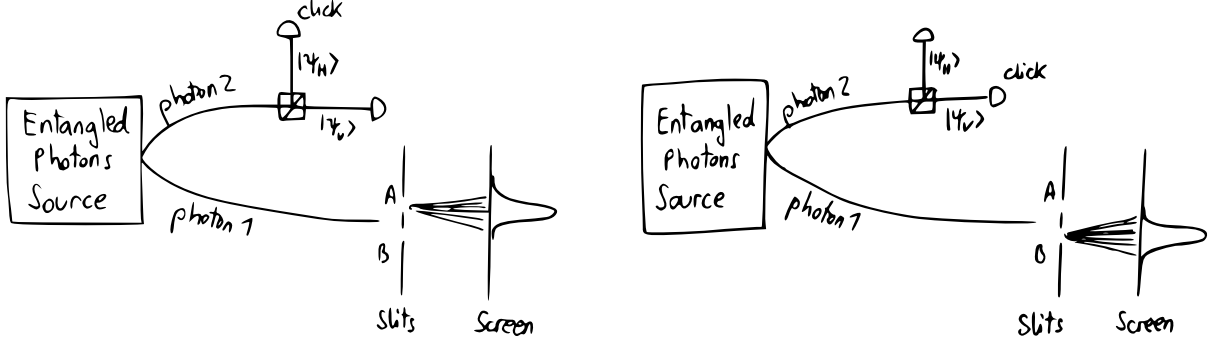


Figure 3.8: Decoherence case. A polarization measurement on photon 2 corresponds effectively to the closure of one slit. Which of the two slits gets closed depends on the result of the measurement.

Dealing the wave function only with spatial degree of freedom, the reduced form for the velocity field (1.10) can be applied and yields:

$$\mathbf{v}_1(\mathbf{q}_1, \mathbf{q}_2) \propto \text{Im} \left[\frac{\nabla_1 \psi_A(\mathbf{q}_1)\psi_H(\mathbf{q}_2) + \nabla_1 \psi_B(\mathbf{q}_1)\psi_V(\mathbf{q}_2)}{\psi_A(\mathbf{q}_1)\psi_H(\mathbf{q}_2) + \psi_B(\mathbf{q}_1)\psi_V(\mathbf{q}_2)} \right]. \quad (3.9)$$

As expected, there are no interference terms guiding the particle evolution. Noticing that either $\psi_H(\mathbf{q}_2) = 0$ or $\psi_V(\mathbf{q}_2) = 0$ by virtue of the assumption (3.6), the two cases of Fig.3.8 arise

manifestly: photon 1 follows either

$$\mathbf{v}_1(\mathbf{q}_1, \mathbf{q}_2) = \mathbf{v}_1(\mathbf{q}_1) \propto \text{Im} \left[\frac{\nabla_1 \psi_A(\mathbf{q}_1)}{\psi_A(\mathbf{q}_1)} \right] \quad (3.10)$$

or

$$\mathbf{v}_1(\mathbf{q}_1, \mathbf{q}_2) = \mathbf{v}_1(\mathbf{q}_1) \propto \text{Im} \left[\frac{\nabla_1 \psi_B(\mathbf{q}_1)}{\psi_B(\mathbf{q}_1)} \right]. \quad (3.11)$$

Thus, the particle is always guided either only by ψ_A or by ψ_B .

3.4.2 Interference

In this case, the second photon is projected into some polarization state, again before photon 1 reaches the slits. This measurement, which does not give any information about the initial polarization state of photon 2, destroys the entanglement between the two photons. Therefore this situation effectively corresponds to the standard case of a particle sent towards a double-slit apparatus when both slits are open. An interference pattern is then observed at the screen (see Fig.3.9).

On account of the consideration above, the relevant wave function for this case is

$$\psi_1(\mathbf{q}_1) = \frac{1}{\sqrt{2}} (\psi_A(\mathbf{q}_1) + \psi_B(\mathbf{q}_1)). \quad (3.12)$$

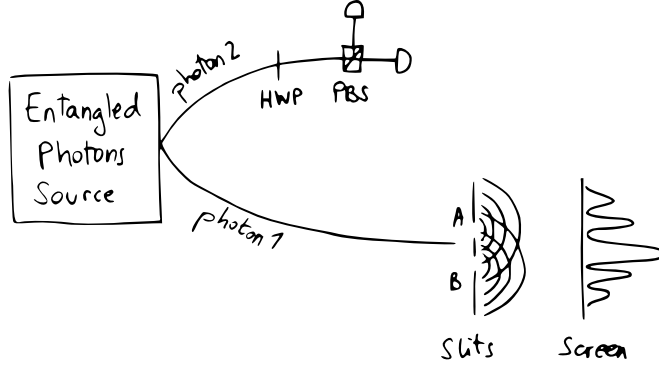


Figure 3.9: Interference case. The initial measurement of photon 2, which destroys the entanglement between the two photons, reduces the situation to the traditional configuration of a single particle in a double-slit.

In the velocity expression

$$\begin{aligned} \mathbf{v}_1(\mathbf{q}_1) &\propto \text{Im} \left[\frac{\psi_1^*(\mathbf{q}_1) \nabla_1 \psi_1(\mathbf{q}_1)}{|\psi_1(\mathbf{q}_1)|^2} \right] \\ &= \text{Im} \left[\frac{\psi_A^*(\mathbf{q}_1) \nabla_1 \psi_A(\mathbf{q}_1) + \psi_B^*(\mathbf{q}_1) \nabla_1 \psi_B(\mathbf{q}_1) + \psi_A^*(\mathbf{q}_1) \nabla_1 \psi_B(\mathbf{q}_1) + \psi_B^*(\mathbf{q}_1) \nabla_1 \psi_A(\mathbf{q}_1)}{|\psi_A(\mathbf{q}_1)|^2 + |\psi_B(\mathbf{q}_1)|^2 + 2 \text{Re}[\psi_A(\mathbf{q}_1) \psi_B^*(\mathbf{q}_1)]} \right], \end{aligned} \quad (3.13)$$

the presence of interference is evident in the phase dependent terms which combine ψ_A and ψ_B .

The reduced form reads:

$$\mathbf{v}_1(\mathbf{q}_1) \propto \text{Im} \left[\frac{\nabla_1 \psi_1(\mathbf{q}_1)}{\psi_1(\mathbf{q}_1)} \right] = \text{Im} \left[\frac{\nabla_1 \psi_A(\mathbf{q}_1) + \nabla_1 \psi_B(\mathbf{q}_1)}{\psi_A(\mathbf{q}_1) + \psi_B(\mathbf{q}_1)} \right]. \quad (3.14)$$

For positions \mathbf{q}_1 in the interference region where both ψ_A and ψ_B are non-vanishing, the photon is guided by both parts of the wave function (3.12).

3.4.3 Surreal Case

The surreal case occurs when the polarization of photon 2 is not measured at all (see Fig.3.10). By the side of photon 1, as described above, the passage through the slits represents a conversion of the polarization degree of freedom into the spatial one. Therefore, while photon 1 travels within the interference region, the total wave function of the system presents entanglement in path-polarization degrees of freedom:

$$|\Psi\rangle = \frac{1}{\sqrt{2}}(|\psi_A\rangle |H\rangle + |\psi_B\rangle |V\rangle). \quad (3.15)$$

The usual projection in real space leaves the wave function in the hybrid notation

$$\Psi(\mathbf{q}_1) = \frac{1}{\sqrt{2}} (\psi_A(\mathbf{q}_1) |H\rangle + \psi_B(\mathbf{q}_1) |V\rangle), \quad (3.16)$$

where photon 2 is still represented by kets of polarization. The Bohmian velocity field (1.9)

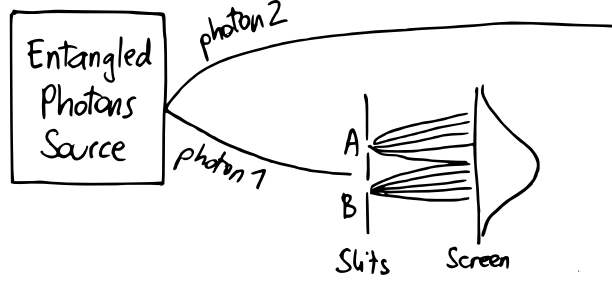


Figure 3.10: Surreal case. The entanglement with the unmeasured photon 2 leads to have both slits open, but no interference.

deriving by this wave function has the form:

$$\begin{aligned} \mathbf{v}_1(\mathbf{q}_1) &\propto \text{Im} \left[\frac{(\psi_A^*(\mathbf{q}_1) \langle H| + \psi_B^*(\mathbf{q}_1) \langle V|) \nabla_1 (\psi_A(\mathbf{q}_1) |H\rangle + \psi_B(\mathbf{q}_1) |V\rangle)}{(\psi_A^*(\mathbf{q}_1) \langle H| + \psi_B^*(\mathbf{q}_1) \langle V|) (\psi_A(\mathbf{q}_1) |H\rangle + \psi_B(\mathbf{q}_1) |V\rangle)} \right] \\ &= \text{Im} \left[\frac{\psi_A^*(\mathbf{q}_1) \nabla_1 \psi_A(\mathbf{q}_1) + \psi_B^*(\mathbf{q}_1) \nabla_1 \psi_B(\mathbf{q}_1)}{|\psi_A(\mathbf{q}_1)|^2 + |\psi_B(\mathbf{q}_1)|^2} \right]. \end{aligned} \quad (3.17)$$

This velocity field depends on both the waves ψ_A and ψ_B originating at the slits, as seen in the interference case (3.14); but at the same time does not show any interference term, as happens in the decoherence case (3.9).

Curiously, the result of the experiment in this configuration is exactly what would be expected from a double-slit experiment in classical terms: both slits are open, but on the screen no interference pattern is expected, rather a trivial sum of the probability distributions of the photons arriving from the two slits as if only one was open at a time. This observation receives a mathematical confirmation when the velocity field (3.17) is rewritten as

$$\begin{aligned} \mathbf{v}_1(\mathbf{q}_1) &\propto \frac{|\psi_A(\mathbf{q}_1)|^2}{|\psi_A(\mathbf{q}_1)|^2 + |\psi_B(\mathbf{q}_1)|^2} \operatorname{Im} \left[\frac{\nabla_1 \psi_A(\mathbf{q}_1)}{\psi_A(\mathbf{q}_1)} \right] + \frac{|\psi_B(\mathbf{q}_1)|^2}{|\psi_A(\mathbf{q}_1)|^2 + |\psi_B(\mathbf{q}_1)|^2} \operatorname{Im} \left[\frac{\nabla_1 \psi_B(\mathbf{q}_1)}{\psi_B(\mathbf{q}_1)} \right] \\ &=: p_A \operatorname{Im} \left[\frac{\nabla_1 \psi_A(\mathbf{q}_1)}{\psi_A(\mathbf{q}_1)} \right] + p_B \operatorname{Im} \left[\frac{\nabla_1 \psi_B(\mathbf{q}_1)}{\psi_B(\mathbf{q}_1)} \right]. \end{aligned} \quad (3.18)$$

The velocity field in the surreal case is indeed a weighted sum of the two single slit fields (3.10) and (3.11). The condition for this to happen is twofold. On one hand, photon 2 is not measured until photon 1 reaches the screen, which let both slits give their contribution (ψ_A and ψ_B). On the other hand, ψ_A and ψ_B are entangled with the two possible polarization states of photon 2, which are orthogonal to each other (3.16). The orthogonality in polarization of the two terms of the entangled state prevents the interference between the two wave functions ψ_A and ψ_B in real space. At the same time, both terms contribute to the guiding of each particle since the wave functions of photon 2 overlap in real space. So the surreal scenario is created, in which the lack of interference is observed, even maintaining the two terms of the total wave function a joint support in configuration space.

3.5 This experiment

The aim of our experiment is the realization of the surreal situation described in 3.4.3 and a consequent deeper investigation of the Bohmian trajectories behaviour in this experimental condition. A conceptually different measurement will be done with respect to the measurement performed by Mahler et al. [7].

Limitation in Mahler's experiment

In Mahler et al.'s implementation of the ideal experiment of ESSW [5], an experimental limitation made it impossible to maintain the entanglement between the two photons while photon 1 was travelling along its "surrealistic" trajectory. In fact, to overcome the problem of a significant background, the events of interest were selected by measuring photon 2 as soon as photon 1 had passed through the double-slit. Performing this measurement, the experimental condition was effectively reduced from a potential surreal case to the decoherence case (Section 3.4.1). Then, the way Mahler et al. used to reconstructed the surrealistic trajectories shown in Fig.3.7 was by means of (3.18): they reconstructed the surreal velocity field as a weighted sum of the two single-slit fields.

Measurement conditions of our experiment

In our experiment, the polarization measurement of photon 2 will be performed only after photon 1 has reached the screen. Performing the which-way measurement at that moment is the authentic implementation of the ideal experiment in which surrealistic trajectories were defined [5]. Moreover, the polarization measurement on photon 2 will be realized in different polarization bases. The final goal is then to study the influence that different measurement settings can have

on the trajectories of photon 1 in the interference region.

The aim of this thesis is the implementation of all what concerns the evolution and the measurement of photon 1. Measurements of the Bohmian trajectories in the region behind the slits are performed in the interference case.

Chapter 4

Creation of the setup

4.1 General description of the setup

The experimental setup which has been built in the course of this thesis is depicted in Fig.4.1. Its first part is the realization of a double-slit apparatus, while its second part is the implementation of a weak measurement.

This setup has been designed for the evolution and the measurement of a single photon of wavelength $\lambda = (780 \pm 3)\text{nm}$. Its characteristics has been chosen in order to fulfil the two following requirements. The Gaussian envelope modulating the interference pattern should be (i) broad enough to contain from 5 to 7 nicely visible interference fringes and (ii) narrow enough to confine the single photon in a small region, in order to enable a high detection efficiency.

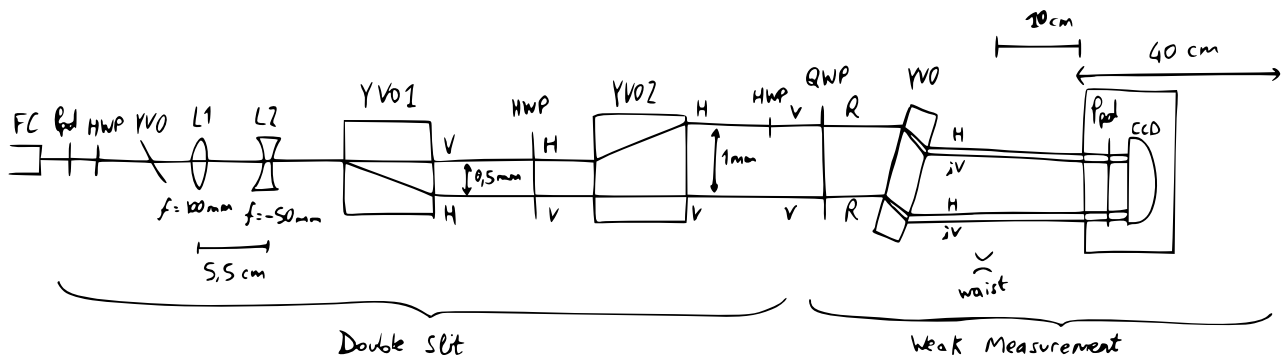


Figure 4.1: Setup of our experiment, schematic representation.

Those requirements have been imposed on the width of the Gaussian modulation at a z position in the far field, where the interference pattern is expected to be observed. This determines the width w_0 of the slits and their reciprocal distance d , as calculated in Appendix A.

In our setup, the width of the slits is the beam waist $w(z)$ at the position z_0 where it reaches its minimum value $w_0 = w(z_0)$. This choice defines z_0 as the effective position of the slits. The value desired in our setup for the slits width is $w_0 \approx 144 \mu\text{m}$.

For the distance d between the slits, on the other hand, a separation $d= 1$ mm has been calculated. This will allow to see 5-7 interference peaks, $390 \mu\text{m}$ far apart one another. The next two sections describe the realization of those two geometrical characteristics of the slits.

Both the preliminary and the final measurements presented here have been performed using a continuous wave laser with wavelength close to the wavelength of the single photon for which the setup has been designed.

4.2 Shaping the Gaussian beam: lenses

A system of lenses is needed to shape the Gaussian beam with the desired minimum waist $w_0 \approx 144 \mu\text{m}$. Moreover, the position z_0 of the minimal waist should be around 30 cm from the last lens because other optical components will be placed between the lens system and the position z_0 of the waist.

The lens in the Fiber Coupler (FC in Fig.4.1) is set such that the beam comes out collimated, with a waist of approximately 1 mm. Thus the absolute position of the lens system from the FC is irrelevant, and what only matters is the choice of the focal length of the lenses and their relative position. A physical reasonable intuition suggested the choice of a biconcave and a biconvex lens. The suitable values of the focal lengths and the relative position has been found via a Mathematica simulation of the problem, implemented in the formalism of matrix optics [50] (see Fig.4.2).

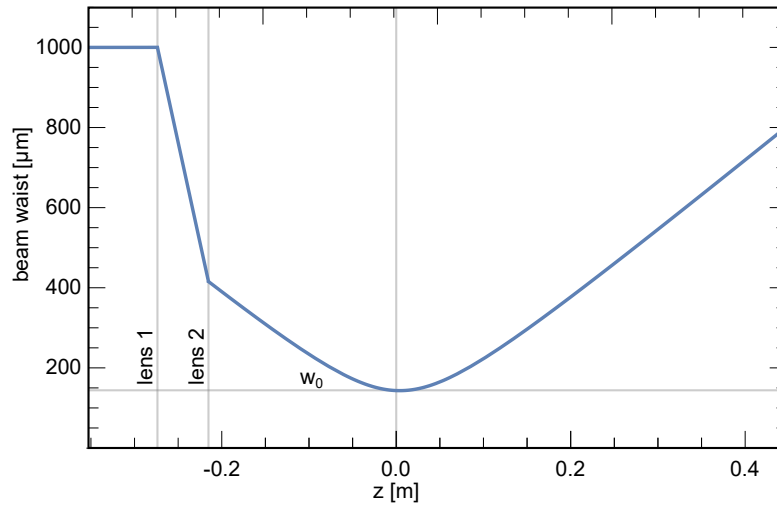


Figure 4.2: Mathematica simulation of the waist evolution in the presence of a biconcave ($f_1= 100$ mm) and a biconvex ($f_2= -50$ mm) lens at a relative distance of 5.5 cm.

Focal lengths of $f_1= 100$ mm and $f_2= -50$ mm have been chosen for the first and the second lens, respectively. A 5.5 cm distance between two such lenses allows to obtain a minimum waist $w_0 \approx 144 \mu\text{m}$ at $z_0 \approx 25$ cm from the second lens. With that system of lenses, the evolution of the waist has been measured in a range of 1.2 m starting from the second lens. The experimental data,

fitted with Eq.A.1, are shown in Fig.4.3. As desired, the experimental waist has its minimum $w_0=143 \mu\text{m}$ at $z_0= 28 \text{ cm}$ far from the second lens.

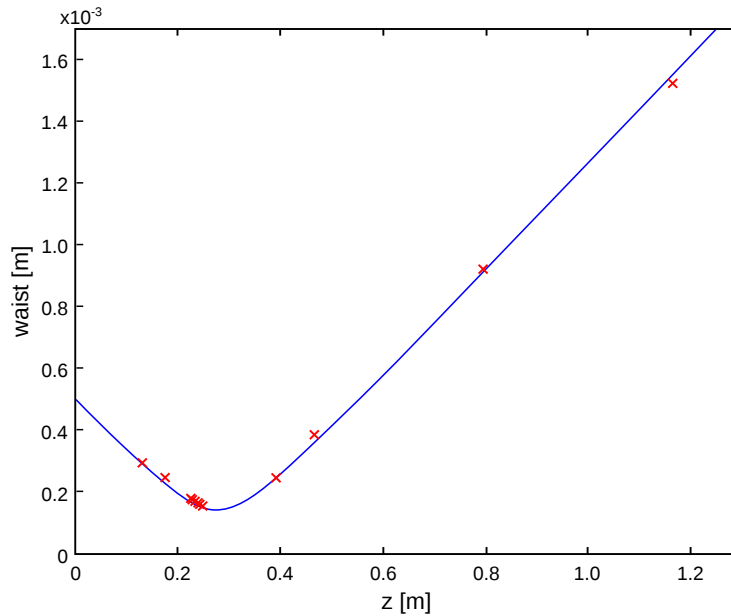


Figure 4.3: Experimental data of the evolution of the beam waist in the presence of a biconcave ($f_1= 100 \text{ mm}$) and a biconvex ($f_2= -50 \text{ mm}$) lens at a relative distance of 5.5 cm. The minimum width is $w_0=143 \mu\text{m}$ at $z_0= 28 \text{ cm}$ from the second lens.

4.3 Birefringent crystals as double-slit

4.3.1 Basic theoretical principles and simulations

In our setup the slits, at least as concerns their separation, are created exploiting the anisotropy of birefringent crystals. In fact, the dynamics of a beam passing through such a crystal is affected by the fact that the physical properties of this medium depend on a specific direction [51]. This characteristic direction, called the optical axis (OA), forms an angle θ_C with the normal to the crystal surface (see Fig4.4).

The OA and the wave vector \mathbf{k} of the beam define a plane. A beam propagating through the crystal is called ordinary beam (o-beam) if its polarization is normal to this plane; extraordinary (e-beam) if its polarization lies in the plane. Entering the crystal, the e-beam is affected by a refractive index (n_e), dependent on the beam polarization and the angle of incidence (θ_1), which is not the same as the refractive index (n_o) that governs the propagation of the o-beam. Therefore, by travelling through a birefringent crystal, two orthogonal polarization components of the same beam get separated¹.

¹The separation concerns the direction of the energy vector \mathbf{S} . The direction of propagation of the wave phase \mathbf{k} , on the other hand, is deflected in the same way for both the o- and the e-beam [51].

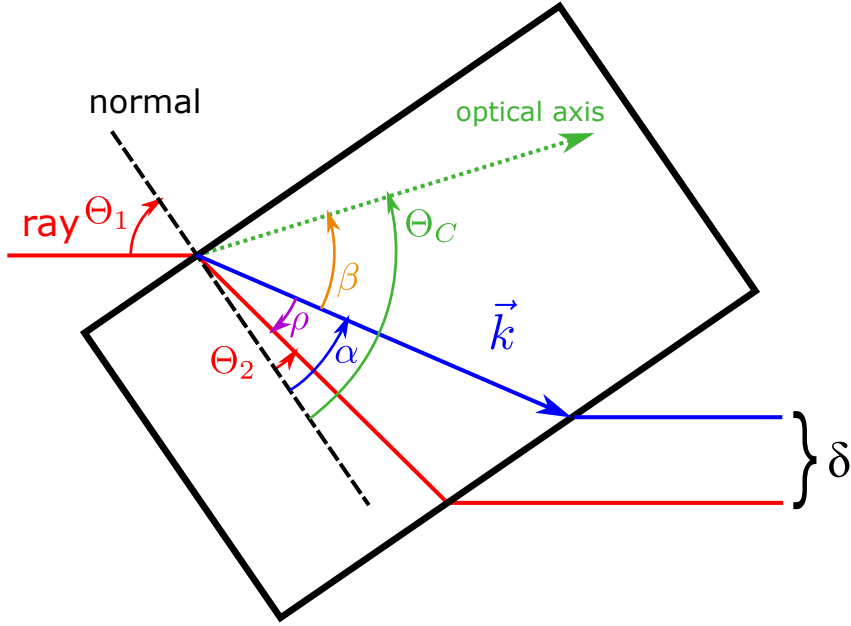


Figure 4.4: Definition of the main parameters of a birefringent crystal.

The distance δ between them at the output face of the crystal is

$$\delta = L \tan \rho, \quad (4.1)$$

where L is the thickness of the crystal and ρ is the “walk-off” angle between the o- and the e-beam (see again Fig.4.4).

This separation δ constitutes in our setup the separation between the two slits. To obtain the desired separation of 1 mm, the behaviour of δ has been studied as a function of the angle of incidence θ_1 , the angle θ_C of the OA, the indices of refraction n_o and n_e , and the thickness of the crystal L . A simulation of the dependence $\delta(\theta_1, \theta_C)$ is shown in Fig.4.5 in the case of a 3.9 cm thick Calcite crystal.

With such a crystal available in the laboratory, the experimental validation of the theoretical prediction has been successfully performed for $\theta_C=45^\circ$ (see Fig.4.6).

4.3.2 Experimental realization

Coarse overlap

In order to obtain interference, the double-slit - besides fulfilling the geometrical constraints discussed at the beginning - must assure a high coherence between the two outgoing beams. The single-crystal double-slit discussed so far presents in this respect a problem. The ordinary and the extraordinary beams, in fact, travelling inside the crystal along different paths, accumulate a pathlength-difference which is in the order of millimeters for a crystal providing the desired 1 mm separation between the beams. This spatial difference between the two wave packets is though much bigger than the coherence length of each packet, $l_c = \frac{2ln(2)}{\pi n} \frac{\lambda^2}{\Delta\lambda} \sim 90 \mu\text{m}$. This prevents the overlap between the wave packets of the two beams, thus leading to decoherence.

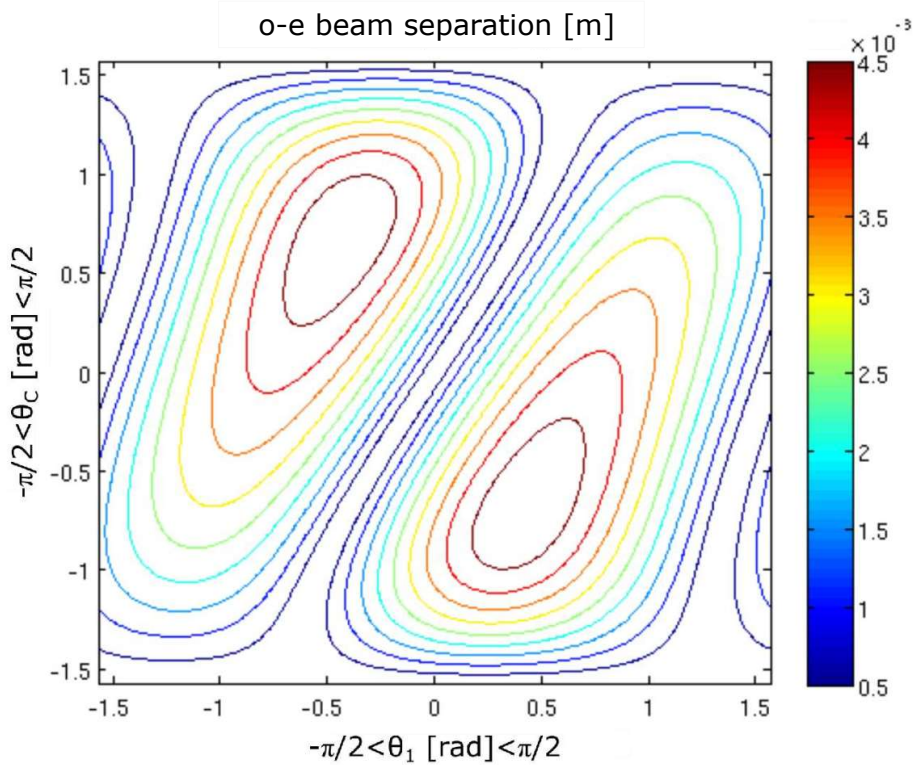


Figure 4.5: Matlab simulation of the separation δ between the ordinary and the extraordinary beams as a function of the incident angle θ_1 and the angle θ_C of the OA. Values calculated for a Calcite crystal with $L=3.9$ cm.

To tackle this issue, a second, identical crystal is placed after the first one, with a half wave plate (HWP) in between to swap the roles of the ordinary and the extraordinary beams (see Fig.4.1). Therefore, the beam which travels the longer path in the first crystal will travel along the shorter in the second crystal, and vice versa for the other beam. Since both beams travel once the long, once the short path, the difference of the pathlengths is coarsely compensated.

For our setup, each of the two birefringent crystals must then create a separation of 0.5 mm between the two beams. Two cubic YVO crystals ($5 \times 5 \times 5 \text{ mm}^3$) with $\theta_C = 90^\circ$ have been chosen for this purpose.

The distance between the two slits created via the two crystals has been measured, as separation between the two beams, directly in front of the slits, where the beams do not interfere yet. The desired 1 mm separation has been achieved, as shown in Fig.4.7.

A fine positioning of the crystals by rotation around the z axis assures that the two beams lie in the same y plane. This ideal condition has been achieved with a precision of $18 \mu\text{m}$. This allows to consider the x and z directions as the only relevant ones.

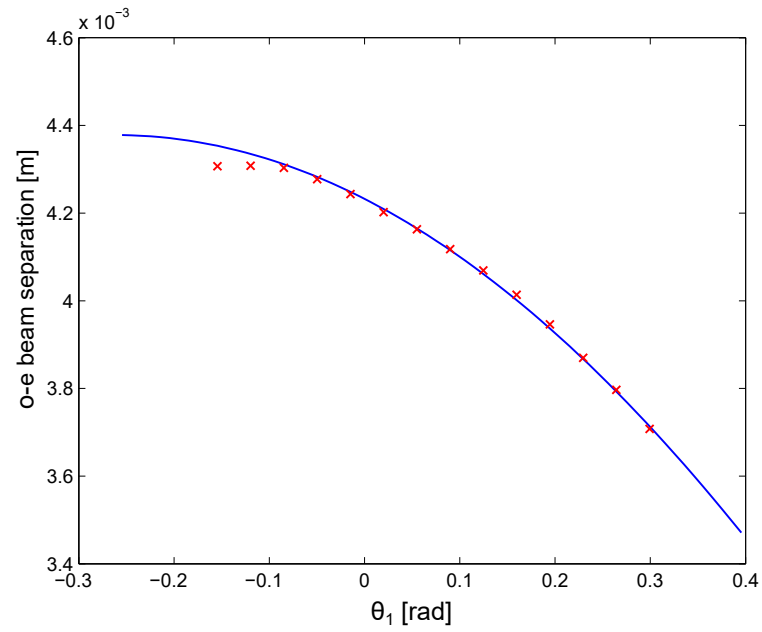


Figure 4.6: Experimental data of the separation δ between the ordinary and the extraordinary beams after a Calcite crystal 3.9 cm thick, studied as a function of the incident angle θ_1 .

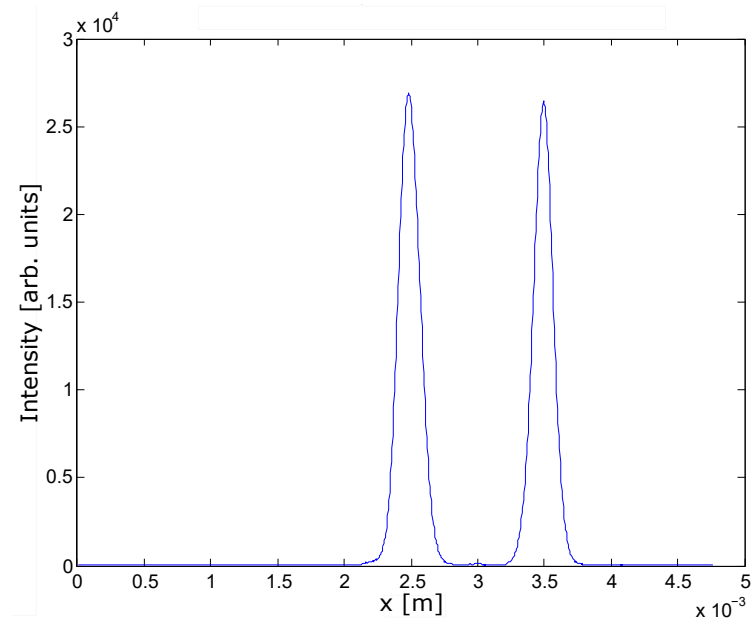


Figure 4.7: Measured intensity profile of the two beams behind the slits. Their separation, corresponding to the distance between the slits, is 1 mm.

Fine overlap

To ensure coherence of the two beams, two more requirements must be fulfilled. First of all, they must have the same polarization. For this purpose, a HWP, specifically designed to act on the H-polarized beam only, is inserted in the setup (see Fig.4.1). The beams coming out from the slits are thus both V-polarized.

Second, the overlap between the two beams must be finer than the coarse pathlength-difference compensation provided by the two-crystals configuration. The finer overlap concerns the single λ peaks inside the Gaussian wave packet. Each of them is $\lambda = (780 \pm 3)\text{nm}$ wide. In order to have the two wavepackets in phase, each inner λ -peak of one packet must overlap with the nearest λ -peak of the other packet with a maximum error set to $\lambda/100$. To achieve such a condition, a high precision is experimentally required in the angular positioning of the crystals. The maximum error for this positioning has been calculated to be around $10\mu\text{rad}$.

In order to achieve this finer overlap condition without turning the slit-crystals themselves (this would change the pathlengths of the beams inside), another YVO is placed in the setup. As shown in Fig.4.1, it has been inserted right before the lenses, just for practical reasons of space. Its small thickness ($L=0.2\text{ mm}$) creates a negligible δ -separation between the different polarization components of the beam, but a relevant phase shift to compensate the small path-length difference. A fine positioning of this YVO makes the two beams exit the second crystal in phase.

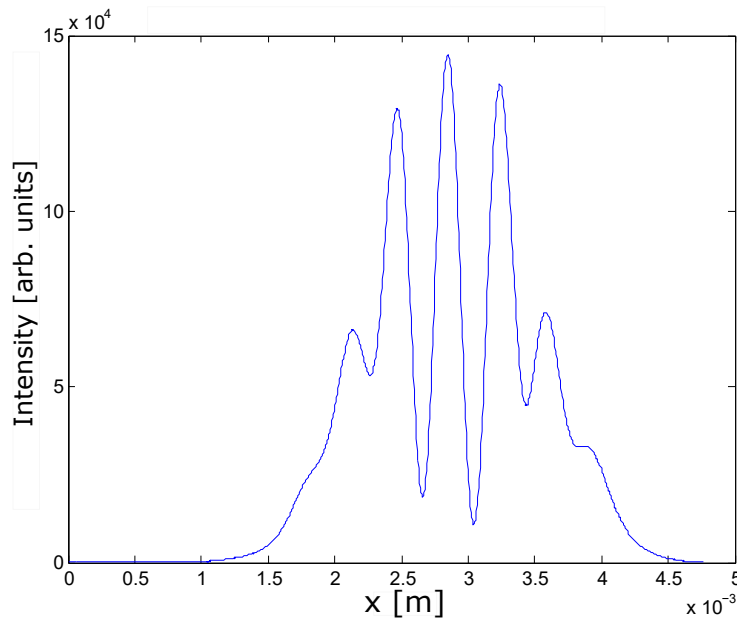


Figure 4.8: Intensity profile of the interference pattern between the two beams in the far field. The separation between two neighbouring interference peaks is $390\mu\text{m}$, as expected.

This coherence condition is at the same time reached and verified by looking for the interference pattern in the far field. When the YVO is rotated to the proper position, the interference pattern is observed in the far field. The two slits are then properly created. In Fig.4.8 the intensity profile in the far field is shown. The distance between two consecutive peaks of interference is $390\mu\text{m}$, as expected from the calculation reported in Appendix A.

4.4 Implementation of the Weak Measurement

The second part of the setup is the implementation of the weak measurement. With it, the Bohmian velocity of photons passing through the double slit will be measured in a range of 40 cm, starting from around 10 cm after the position of the waist.

The measurement apparatus for this weak measurement is the particle itself. Its polarization plays the role of the pointer variable.

Note that, in contrast to the situation presented in Chapter 2, in which the set of eigenvalues was continuous for the pointer variable and discrete for the measured observable, here it is the other way round. The pointer variable, as said, the polarization, has a set of two possible eigenvalues $\{\pm 1\}$, while the measured observable, the momentum of the photon, has a continuous spectrum. The same calculation presented in Chapter 2 can be applied here, keeping in mind the swapping of the roles.

4.4.1 Description of the measurement

As shown in Fig.4.1, the weak measurement is implemented via four optical components, which, in turn, modify the beam. The modification introduced by each of them will be shown by looking at the beam profile at a fixed position, imagining to place the components in the setup one by one. The position at which the beam profile will be observed is chosen in the interference region, about 50 cm after the effective position of the slits.

Quarter Wave Plate (QWP)

The first optical component we place in the optical path after the double slit is a quarter wave plate (QWP), to prepare the polarization pointer state. The QWP rotates the polarization of the photon from the state $|V\rangle$ (as it comes out from the slits) to a circular polarization state, say $|R\rangle = \frac{1}{\sqrt{2}}(|H\rangle + i|V\rangle)$ to make the reasoning concrete.

The beam profile in the interference region looks as sketched in Fig.4.9.

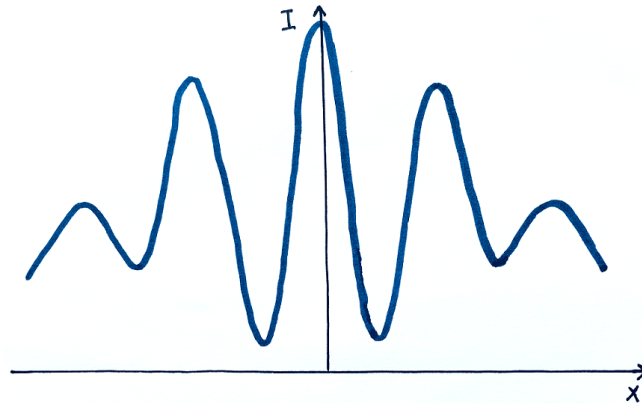


Figure 4.9: Beam profile at 50 cm far from the slits when only the QWP is placed after the slits.

YVO crystal

Then we insert the YVO crystal to couple the momentum of the photon \hat{p} (the system observable) to its polarization (the pointer variable). The corresponding Hamiltonian describing the coupling interaction (2.1) here reads

$$H = \epsilon \hat{p} \otimes \hat{\sigma}_z, \quad (4.2)$$

where the coupling strength ϵ depends on the tilt of the crystal: the smaller the tilt, the weaker the coupling.

As a birefringent crystal, the YVO separates the incoming beam into two beams with orthogonal polarizations (see Fig.4.10). Being our YVO described by the operator $\hat{\sigma}_z$, as in (4.2), means that the two outgoing beams have horizontal and vertical polarization respectively, with a relative phase (in our case fixed to i) depending on both the specific state of the ingoing beam and the fine tilt of the crystal. The distance between the two profiles equals 2ϵ and depends on the coarse tilt of the YVO and its thickness ($L=4.52$ mm). In our case this separation is about $14.3 \mu\text{m}$.

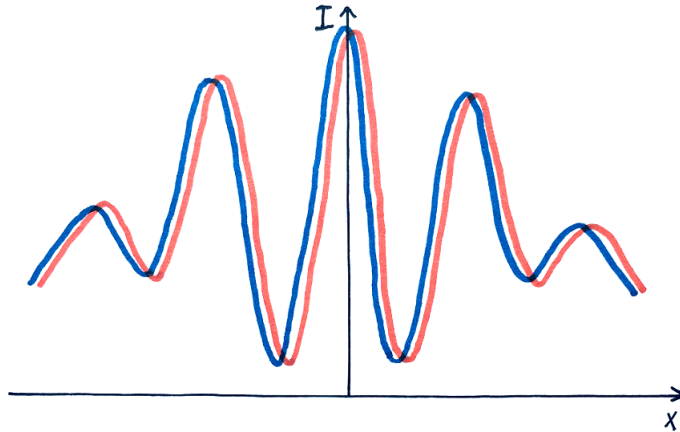


Figure 4.10: Beam profile at 50 cm distance from the slits when QWP and YVO are placed after the slits. The blue profile shows the H-polarized term of (4.3) and the red profile the V-polarized one. The shift between the two profiles is $2\epsilon \approx 14.3 \mu\text{m}$.

The intensity profile shown in Fig.4.10 is the modulo squared of the total wave function (2.7), where the projection onto $\langle q|$ corresponds to the selection of the z plane at which the beam profile is observed. In our case this wave function reads

$$\langle q|\Psi_F\rangle = \frac{1}{\sqrt{2}} [\psi_S(q - \epsilon)|H\rangle + i\psi_S(q + \epsilon)|V\rangle]. \quad (4.3)$$

To obtain it from (2.7), the operator $\hat{\sigma}_z$ and the state $|R\rangle$ have been expressed in the basis of linear polarization $\{|H\rangle, |V\rangle\}$, namely $\hat{\sigma}_z = |H\rangle\langle H| - |V\rangle\langle V|$ and $|R\rangle = \frac{1}{\sqrt{2}}(|H\rangle + i|V\rangle)$.

Note that in (4.3) the spatial function in the two orthogonally polarized terms is slightly shifted in position (to the left in one term and to the right in the other). This is manifestly the correlation (4.2) of momentum, the generator of spatial translations, with polarization.

Polarizer

The momentum-polarization entangled state produced by the YVO is then sent through a polarizer to implement a projective measurement of the pointer variable. This measurement of polarization is performed, in our setup, in the $\{|P\rangle, |M\rangle\}$ basis², which corresponds to a measurement of the operator $\hat{\sigma}_x$.

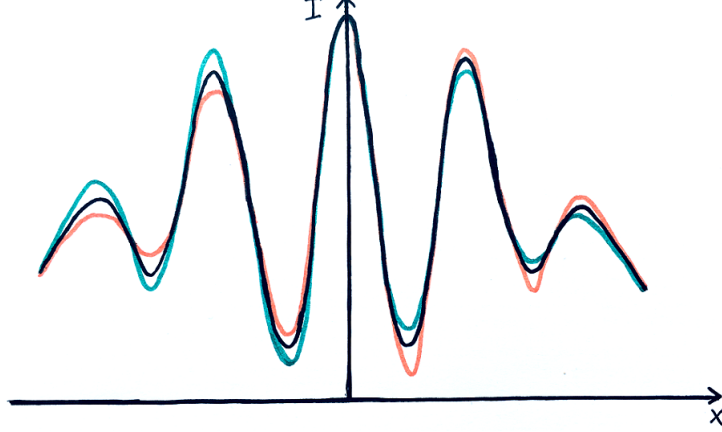


Figure 4.11: Beam profiles at 50 cm far from the slits when QWP, YVO and a polarizer are placed after the slits. The green profile is recorded in presence of a P-polarizer, while the orange one corresponds to the M-polarized beam. The difference between the two profiles leads to the weak value of the photon momentum. As a reference, half of the total intensity of the distribution without any projective measurement is represented in the black curve.

When a P-polarizer is placed in the setup, the momentum-polarization entangled state is projected onto $|P\rangle = \frac{1}{\sqrt{2}}(|H\rangle + |V\rangle)$, yielding the probability (green in Fig.4.11)

$$\begin{aligned} p_P(q) &= |\langle P|\Psi_F\rangle(q)|^2 = \left| \frac{1}{2}(\langle H| + \langle V|)(\psi_S(q - \epsilon)|H\rangle + i\psi_S(q + \epsilon)|V\rangle) \right|^2 \\ &= \frac{1}{4} [|\psi_S(q - \epsilon)|^2 + |\psi_S(q + \epsilon)|^2 + 2\text{Im}[\psi_S(q - \epsilon)\psi_S^*(q + \epsilon)]] . \end{aligned} \quad (4.4)$$

When, on the other hand, a M-polarizer is inserted, the projection is performed onto $|M\rangle = \frac{1}{\sqrt{2}}(|H\rangle - |V\rangle)$ and the probability $p_M(q)$ is equivalently obtained (orange in Fig.4.11)

$$p_M(q) = \frac{1}{4} [|\psi_S(q - \epsilon)|^2 + |\psi_S(q + \epsilon)|^2 - 2\text{Im}[\psi_S(q - \epsilon)\psi_S^*(q + \epsilon)]] . \quad (4.5)$$

From these probabilities the expectation value of $\hat{\sigma}_x$ on $|\Psi_F\rangle$ can be calculated as

$$\langle \hat{\sigma}_x \rangle = \frac{p_P - p_M}{p_P + p_M} = \frac{2\text{Im}[\psi_S(q - \epsilon)\psi_S^*(q + \epsilon)]}{|\psi_S(q - \epsilon)|^2 + |\psi_S(q + \epsilon)|^2} . \quad (4.6)$$

The condition of weak coupling allows the Taylor expansion of $\psi_S(q \pm \epsilon)$ around q :

$$\psi_S(q \pm \epsilon) = \psi_S(q) \pm \partial_q \psi_S(q)\epsilon + \mathcal{O}(\epsilon^2) . \quad (4.7)$$

²Other choices of polarization basis for this measurement and of the initial pointer state are discussed in Appendix B.

With this expansion of $\psi_S(q \pm \epsilon)$ until first order in ϵ , (4.6) reads

$$\begin{aligned} \langle \hat{\sigma}_x \rangle &\approx \frac{2\epsilon \text{Im}[\psi_S(q) \partial_q \psi_S^*(q) - \psi_S^*(q) \partial_q \psi_S(q)]}{2|\psi_S(q)|^2} = \epsilon \frac{\text{Im}[-2i \text{Im}[\psi_S^*(q) \partial_q \psi_S(q)]]}{|\psi_S(q)|^2} \\ &= -2\epsilon \frac{\text{Im}[\psi_S^*(q) \partial_q \psi_S(q)]}{|\psi_S(q)|^2}, \end{aligned} \quad (4.8)$$

which can be recognized as the Bohmian velocity (1.9).

CCD camera

The CCD camera, always implicitly considered so far when showing the intensity profiles, is used to perform a strong measurement of position. This final measurement corresponds to the post-selection.

The camera is mounted on a translation stage which scans the z direction from 12.5 to 52.5 cm after the slits. Moving the camera within this range allows to extract the weak value of momentum for different position of the interference region. From this vector field of velocity the possible trajectories can be reconstructed.

4.4.2 YVO crystal as entangling medium

Momentum of the wave function and Bohmian velocity of the particle

As shown in Eq.(4.2), $\hat{H}_I = \epsilon \hat{p} \otimes \hat{\sigma}_z$, the YVO in our setup provides the entanglement between the system and the apparatus necessary in any measurement process (Section 2.21). In our measurement, the degree of freedom of the apparatus is polarization ($\hat{\sigma}_z$), whereas the system observable is the momentum \hat{p} of the wave function.

Note, however, that what we are interested to extract from our measurement is not that momentum \hat{p} of the wave function, but rather the Bohmian velocity v_B of the particle. It is obtained, as a weak value, with a weak measurement of \hat{p} *and* a further postselection of the position q (see Section 2.21).

Thus \hat{p} and v_B are indeed two distinct physical entities. In particular, while v_B changes at different positions of the interference region (thence the not straight Bohmian trajectories), the momentum \hat{p} is a constant of motion. In the interference region, in fact, the spatial wave function evolves accordingly to the free space Hamiltonian \hat{H}_{free} , with which the momentum \hat{p} commutes: $[\hat{H}_{\text{free}}, \hat{p}] = 0$.

Entangling interaction and time evolution

Let us consider now the entangled state created by the YVO: $|\Psi_F\rangle = \frac{1}{\sqrt{2}} [|\psi_S^1\rangle |H\rangle + i |\psi_S^2\rangle |V\rangle]$ (state (4.3) before the expansion in q -representation). The time evolution it undergoes is governed by the Hamiltonian $\hat{H}_{\text{ev}} = \hat{H}_{\text{free}} \otimes \mathbb{1}$. Since this Hamiltonian has the form of a tensor product, the entanglement is preserved over time.

Another favourable property of the time evolution Hamiltonian \hat{H}_{ev} is the commutation with the interaction Hamiltonian:

$$[\hat{H}_{\text{ev}}, \hat{H}_I] = 0. \quad (4.9)$$

This physically means that the entangling process necessary for the measurement can be done at any time of the time evolution of the system.

The experimental counterpart of (4.9) is the legitimacy to place the entangling YVO at any position of the interference region, of course before the position of the postselection (it is evident that a convenient position is right in front of the slits, which provides entanglement at any position of the entire interference region).

The freedom in the choice of the YVO position can be also intuitively seen from the following fact. What the YVO effectively does is creating a spatial separation between the two components of the wave function correlated with orthogonal polarizations (Eq.4.3 and Fig.4.10). Thanks to this separation, the Bohmian velocity can be extracted from the intensity profiles as described in the previous Section. The constant amount of this separation, 2ϵ , is evidently independent of the position at which the YVO is placed.

Chapter 5

Measurement results

5.1 Realistic initial pointer state

Some deviations from the ideal measuring condition described in the previous chapter have been of course detected in our measurement. The initial state of the pointer variable represents the most interesting one. The polarization of the laser beam has in fact been found to be not in a perfectly circularly polarized state. Rather, an excess of P-polarization component has been detected over the M-polarization one. The information of the initial polarization state has been

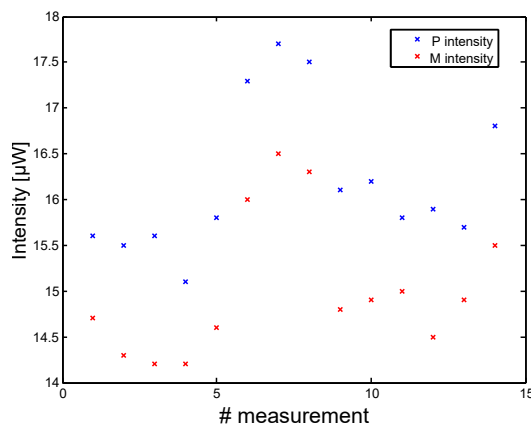


Figure 5.1: The slight excess of P-polarized light with respect to M makes the initial pointer state not exactly circularly polarized.

obtained by a set of intensity measurements. Pairs of P and M intensity values have been recorded within a time interval shorter than the characteristic time of laser fluctuations (see Fig.5.1).

The deviation of the initial pointer state from the ideal case $\langle \hat{\sigma}_x \rangle_0^{ideal} = 0$ amounts to 3.8%, which is still considerably close to the required circularly polarized state (see Appendix B). According to the measurement procedure explained in Chapter 2, the shift of the pointer state from this value has been considered as measurement result.

The intensity ratio $P/M \approx 1.08 \pm 0.02$ as been taken into account in the crucial analysis of the relative intensity between the P and M profiles.

5.2 Average trajectories of photons

The beam profile has been measured in the range from 12.5 to 52.5 cm after the double slit at 41 equidistant imaging planes. For each plane, a set of 5 P-polarized profiles and 5 M-polarized profiles have been recorded. Averaging over them as required by the weak measurement method, a pair of P- and M-polarized profiles has been obtained for each imaging plane.

From each such pair the momentum of the photons has been calculated for various x position of the corresponding z plane. As expected, most of the momentum is in the longitudinal direction, $k_z = \frac{2\pi}{\lambda} \approx 8 \cdot 10^6 \text{ m}^{-1}$, while the transversal momentum is orders of magnitude smaller: $|k_x| < 5 \cdot 10^4 \text{ m}^{-1}$.

The transversal momentum calculated from the data at the $z = 30 \text{ cm}$ imaging plane behind the double slit is represented in Fig.5.2. Note the symmetrical behaviour with respect to the origin of the x axis.

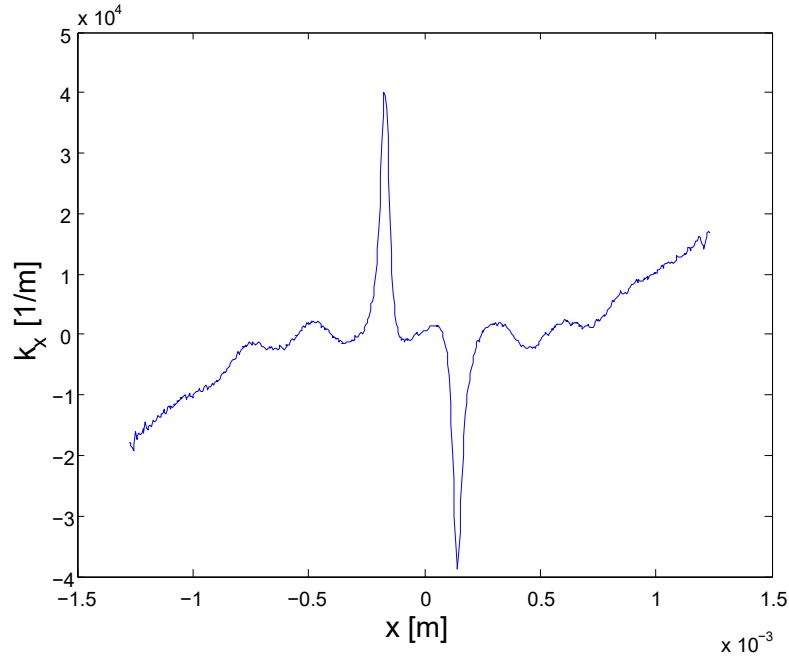


Figure 5.2: Transversal photon momentum recorded at the $z = 30 \text{ cm}$ imaging plane behind the double slit.

By interpolation between the various imaging planes, the entire 2D velocity field has been reconstructed. As boundary condition to the deterministic evolution problem, the probability distribution of the photon position at the middle point of the scanned z range has been provided. From those information, the average Bohmian trajectories of photons have been obtained.

In Fig.5.3, 80 possible trajectories of photons in a double slit apparatus are shown. As expected from previous discussion (Section 3.1.2), the Bohmian trajectories do not cross each other and show a symmetric behaviour with respect to the $x = 0$ axis.

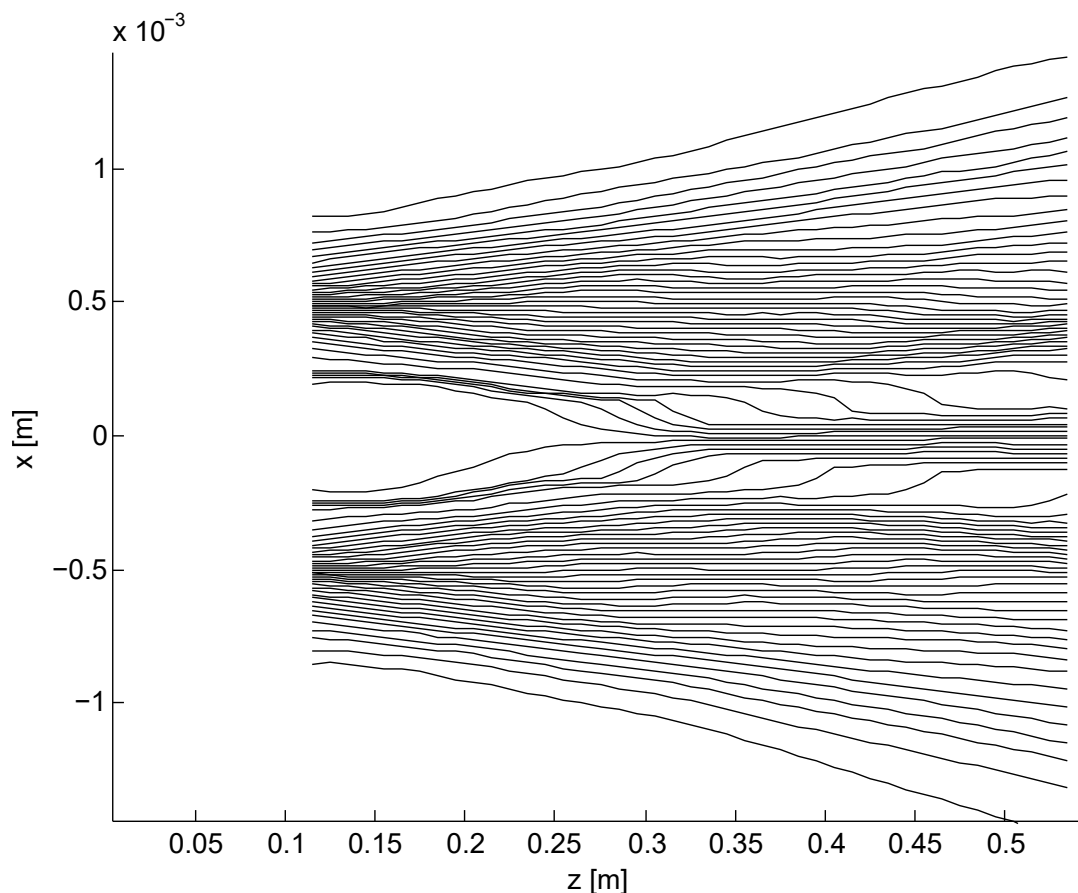


Figure 5.3: Average trajectories of photons in a double slit interferometer, reconstructed by measured data.

Moreover, an increasing density of trajectories is nicely visible in correspondence of the three central interference peaks. In the Bohmian explanation of the double-slit experiment, in fact, particle trajectories are describable while retaining the interference pattern.

The average trajectories obtained in this thesis with a classical continuous-wave laser source resemble the single-photons average trajectories recorded by Kocsis et al. [46], presented in Section 3.2. The observation of such an analogous behaviour is an experimental demonstration of the proposal of Bliokh et al. [44] to give a classical interpretation to Kocsis' single-photons average trajectories. After all, the weak measurement performed by Kocsis et al. inevitably requires averaging over many single-photons events. As a result of such averaging process, “the single-photon or multi-photon character of the field does not make any difference” [44].

The significance of average photons trajectories reconstructed by the method of weak measurements is still to be understood more deeply. Although the Bohmian velocity is defined as a weak value (Section 2.4), the inevitable averaging process required by the weak measurement method makes the identification of the reconstructed trajectory with the desired single particle trajectory not straightforward any longer. When this measurement procedure is applied in a

single-photon regime, is it still legitimate to ascribe the result obtained by averaging over an ensemble of many quantum particles to a single particle? If this is not the case, then the Bohmian single particle trajectories remain just an intuitive picture for the description of the dynamics of quantum particles. In this scenario, the measured “average trajectories” can be still regarded as the streamlines of the probability current.

Conclusions

A deeper investigation of the non-local character of Bohmian mechanics has inspired our experiment, based on pairs of entangled photons and a double-slit apparatus.

In this thesis project an optical double-slit apparatus has been created with a design suitable for a single photon of $\lambda \approx 780$ nm. With a continuous-wave laser of the same wavelength, the proper operation of the double-slit setup has been tested.

Afterwards, Bohmian trajectories of photons in the interference region of this double-slit apparatus were observed. The eventual investigation of Bohmian non-locality will be in fact based on the behaviour of such single-photon trajectories. To this aim, a weak measurement of photon momentum has been implemented. With it, the photon velocity field has been scanned in a 40 cm range of the interference region.

From the measured velocity field, average trajectories of photons have been reconstructed. As expected from the Bohmian theory, our measured trajectories do not cross each other and show a clear symmetry with respect to the optical axis of the setup. At the same time, the interference pattern is still recognisable by the density of the trajectories, which increases in correspondence to the interference peaks.

Moreover, the behaviour of our trajectories obtained with a classical light source is totally equivalent to the one of the weakly measured average trajectories recorded by Kocsis et al. [46] in a regime of single photons. This analogy provides a qualitative experimental proof to the classical interpretation of Kocsis et al.'s experiment, as suggested by Bliokh et al. [44]. According to this interpretation in fact, averaging over many single-photons events, as required by the weak measurement method, is nothing else but a multi-photon limit of classical linear optics.

The real nature of Bohmian trajectories and the significance of the results extracted by a process of averaging are still under investigation.

With the results achieved in this thesis, the largest part of a new setup is ready. With our final experiment, new insights on the non-local character of Bohmian mechanics will be provided. To the Bohmian theory a challenge will be given for the explanation of new results, but at the same time also a chance for its further development.

Appendix A

Definition of the geometrical parameters of the slits

The geometrical parameters of a double-slit created via a Gaussian beam are based on the waist w of the beam. It evolves along the direction of propagation z according to

$$w(z) = w_0 \sqrt{1 + \left(\frac{z}{z_R}\right)^2}, \quad (\text{A.1})$$

where the Rayleigh length z_R , defined as

$$z_R = \frac{\pi w_0^2}{\lambda}, \quad (\text{A.2})$$

is the maximum distance from z_0 at which the plane wave approximation is still valid.

Width w_0

In our experimental conditions, it is suitable to have the interference pattern at $z \approx 50$ cm behind the slits. That means, this z position must lie in the far field of the slits.

For our Gaussian beam this conditions corresponds to $R = \frac{z}{z_R} \gg 1$, let us say $R=6$.

For those values of z and R , the value of the minimum waist (the width of the slits) is

$$w_0 = \sqrt{\frac{z\lambda}{\pi R}} = 144 \mu\text{m}. \quad (\text{A.3})$$

Distance d

The distance d between the slits depends on both the width of the Gaussian at the position $z=50$ cm and the number of peaks one wishes to see in it.

To estimate the visible width of the Gaussian (theoretically infinite) let us assume that the signal is usable until the envelope drops to 1% of its maximal intensity. Defining f as the threshold value, $f=0.01$, the assumption reads:

$$f = e^{-\frac{2x^2}{w(z)^2}}, \quad (\text{A.4})$$

where x_V is half of the visible waist. Thus, the total visible waist at $z=50$ cm is

$$2x_V = 2\sqrt{\ln 1/f} \frac{w(z)}{\sqrt{2}} \approx 2.7 \text{ mm.} \quad (\text{A.5})$$

To fulfil the requirement of having about 7 visible peaks within $2x_V$, the interference peaks must be $390 \mu\text{m}$ far apart one another. Considering that the distance between the interference peaks produced by a double-slit apparatus is $\frac{z\lambda}{d}$, the distance d between the slits is determined to be $d=1$ mm.

Appendix B

Discussion of alternative setups

In this Appendix, possible variations of our setup are discussed with respect to the choice of the initial pointer state (the measurement apparatus state $|\psi_M\rangle$) and the polarization basis onto which the pointer state is eventually projected.

The Hamiltonian (4.2) is kept the same throughout the discussion. This corresponds to keeping always the same YVO which splits the incoming beam into two beams, each one being an eigenstate of $\hat{\sigma}_z$.

Let us start considering an eigenstate of $\hat{\sigma}_z$ as the initial $|\psi_M\rangle$, for example $|H\rangle$ (an analogous discussion holds also for $|V\rangle$).

In this case, (4.3) simply reads

$$\langle q | \Psi_F \rangle = \psi_S(q - \epsilon) |H\rangle. \quad (\text{B.1})$$

Being $|\psi_M\rangle$ an eigenstate of the YVO, just one beam comes out from the crystal. Thence the failure of the $|H\rangle/|V\rangle$ choice. In fact, since the probabilities of the P/M polarization measurement on (B.1) are $p_P = p_M$, the expectation value of $\hat{\sigma}_x$ on (B.1) yields a useless $\langle \hat{\sigma}_x \rangle = 0$. The same for $\langle \hat{\sigma}_y \rangle$.

On the contrary, the choice of an eigenstate of $\hat{\sigma}_x$, $|P\rangle$ or $|M\rangle$, as initial pointer state makes the measurement possible, as long as the final polarization measurements are performed in the $\hat{\sigma}_y$ basis.

Let us consider $|\psi_M\rangle = |P\rangle$. The corresponding state after the YVO in q representation (4.3) reads:

$$\langle q | \Psi_F \rangle = \frac{1}{\sqrt{2}} [\psi_S(q - \epsilon) |H\rangle + \psi_S(q + \epsilon) |V\rangle]. \quad (\text{B.2})$$

With analogous calculations as the ones which led to (4.8), the result of a measurement of $\hat{\sigma}_y$ on that state can be proven to be

$$\langle \hat{\sigma}_y \rangle \approx 2\epsilon \frac{\text{Im}[\psi^*(q) \partial_q \psi(q)]}{|\psi(q)|^2}. \quad (\text{B.3})$$

While measuring $\hat{\sigma}_x$ onto (B.2) would uselessly yield $\langle \hat{\sigma}_x \rangle = 1$.

The same holds similarly when choosing an eigenstate of $\hat{\sigma}_y$ as initial pointer state. Analogously as demonstrated above, one can see that with $|\psi_M\rangle = |\bar{R}\rangle$ or $|L\rangle$, as in our setup, the only possibility to get meaningful results is measuring the polarization in the $\hat{\sigma}_x$ basis.

Bibliography

- [1] David Bohm. *Quantum Theory*. Prentice-Hall Physics Series, New York, 1951.
- [2] Jun John Sakurai. *Modern quantum mechanics; rev. ed.* Reading, MA: Addison-Wesley, 1994. URL: <https://cds.cern.ch/record/1167961>.
- [3] David Bohm. “A Suggested Interpretation of the Quantum Theory in Terms of "Hidden" Variables. I”. In: *Phys. Rev.* 85 (2 Jan. 1952), pp. 166–179. DOI: 10.1103/PhysRev.85.166. URL: <https://link.aps.org/doi/10.1103/PhysRev.85.166>.
- [4] David Bohm. “A Suggested Interpretation of the Quantum Theory in Terms of "Hidden" Variables. II”. In: *Phys. Rev.* 85 (2 Jan. 1952), pp. 180–193. DOI: 10.1103/PhysRev.85.180. URL: <https://link.aps.org/doi/10.1103/PhysRev.85.180>.
- [5] B. Englert et al. “Surrealistic Bohm Trajectories”. In: *Zeitschrift für Naturforschung* 47a (1992), pp. 1175–1186. DOI: 10.1515/zna-1992-1201.
- [6] Howard Wiseman. “Grounding Bohmian Mechanics in Weak Values and Bayesianism”. In: 9 (June 2007), p. 165.
- [7] Dylan H. Mahler et al. “Experimental nonlocal and surreal Bohmian trajectories”. In: *Science Advances* 2.2 (2016). DOI: 10.1126/sciadv.1501466. URL: <http://advances.sciencemag.org/content/2/2/e1501466>.
- [8] Sheldon Goldstein. “Bohmian Mechanics”. In: *The Stanford Encyclopedia of Philosophy*. Ed. by Edward N. Zalta. Summer 2017. Metaphysics Research Lab, Stanford University, 2017.
- [9] Christopher A. Fuchs and Asher Peres. “Quantum Theory Needs No ‘Interpretation’”. In: *Physics Today* 53 (3 Mar. 2000), pp. 70–71. DOI: 10.1063/1.883004.
- [10] D. Bohm, B.J. Hiley, and P.N. Kaloyerou. “An ontological basis for the quantum theory”. In: *Physics Reports* 144.6 (1987), pp. 321–375. ISSN: 0370-1573. DOI: [https://doi.org/10.1016/0370-1573\(87\)90024-X](https://doi.org/10.1016/0370-1573(87)90024-X). URL: <http://www.sciencedirect.com/science/article/pii/037015738790024X>.
- [11] D. Dürr et al. “Bohmian Mechanics”. In: *ArXiv e-prints* (Mar. 2009). arXiv: 0903.2601 [quant-ph].
- [12] John S. Bell. “On the Problem of Hidden Variables in Quantum Mechanics”. In: *Rev. Mod. Phys.* 38 (3 July 1966), pp. 447–452. DOI: 10.1103/RevModPhys.38.447. URL: <https://link.aps.org/doi/10.1103/RevModPhys.38.447>.
- [13] J. S. Bell and Alain Aspect. *Speakable and Unspeakable in Quantum Mechanics: Collected Papers on Quantum Philosophy*. 2nd ed. Cambridge University Press, 2004. DOI: 10.1017/CB09780511815676.

- [14] Nino Zanghí. *David Joseph Bohm: Un fisico teorico ignorato*. Colloquium in Aula Rostagni, Università di Padova. Apr. 2017.
- [15] John Stewart Bell. “Towards an exact quantum mechanics”. In: (1989). URL: <https://cds.cern.ch/record/209780>.
- [16] John von Neumann. *Mathematische Grundlagen der Quantenmechanik*. Springer-Verlag Berlin Heidelberg, 1932. DOI: 10.1007/978-3-642-61409-5.
- [17] Boris Braverman and Christoph Simon. “Proposal to Observe the Nonlocality of Bohmian Trajectories with Entangled Photons”. In: *Phys. Rev. Lett.* 110 (6 Feb. 2013), p. 060406. DOI: 10.1103/PhysRevLett.110.060406. URL: <https://link.aps.org/doi/10.1103/PhysRevLett.110.060406>.
- [18] John S. Bell. “On the Einstein-Podolsky-Rosen paradox”. In: *Physics* 1 (1964), pp. 195–200.
- [19] Detlef Dürr and Stefan Teufel. *Bohmian Mechanics*. Springer, Berlin, Heidelberg, 2009. DOI: 10.1007/978-3-540-89344-8.
- [20] Detlef Dürr et al. “Comment on "Surrealistic Bohm Trajectories"”. In: *Zeitschrift für Naturforschung A* 48 (Dec. 1993).
- [21] E. Madelung. “Quantentheorie in Hydrodynamischer Form”. In: *Z. Physik* 40 (1926), pp. 322–326. DOI: 10.1007/BF01400372.
- [22] C. Philippidis, C. Dewdney, and B.J. Hiley. “Quantum interference and the quantum potential”. In: *Nuov Cim B* 52 (July 1979), pp. 15–28. ISSN: 1826-9877. DOI: 10.1007/BF02743566.
- [23] D. Bohm and B.J. Hiley. “Measurement understood through the quantum potential approach”. In: *Foundations of Physics* 14 (3 Mar. 1984), pp. 255–274. DOI: 10.1007/bf00730211.
- [24] D. Dürr, S. Goldstein, and N. Zanghí. “Quantum equilibrium and the origin of absolute uncertainty”. In: *Journal of Statistical Physics* 67 (June 1992), pp. 843–907. DOI: 10.1007/BF01049004. eprint: [quant-ph/0308039](http://arxiv.org/abs/quant-ph/0308039).
- [25] Max Born. “Zur Quantenmechanik der Stoßvorgänge”. In: *Zeitschrift für Physik* 37.12 (1926), pp. 863–867.
- [26] H. D. Zeh. “Why Bohm’s Quantum Theory?” In: *Foundations of Physics Letters* 12 (Apr. 1999). DOI: 10.1023/A:1021669308832. eprint: [quant-ph/9812059](http://arxiv.org/abs/quant-ph/9812059).
- [27] B J Hiley and R E Callaghan. “Delayed-choice experiments and the Bohm approach”. In: *Physica Scripta* 74.3 (2006), p. 336. URL: <http://stacks.iop.org/1402-4896/74/i=3/a=007>.
- [28] B. J. Hiley, R. E Callaghan, and O. Maroney. “Quantum trajectories, real, surreal or an approximation to a deeper process?” In: *eprint arXiv:quant-ph/0010020* (Oct. 2000). eprint: [quant-ph/0010020](http://arxiv.org/abs/quant-ph/0010020).
- [29] Marlan O Scully. “Do Bohm trajectories always provide a trustworthy physical picture of particle motion?” In: *Physica Scripta* 1998.T76 (1998), p. 41. URL: <http://stacks.iop.org/1402-4896/1998/i=T76/a=005>.
- [30] R. P. Feynman. “Space-Time Approach to Non-Relativistic Quantum Mechanics”. In: *Rev. Mod. Phys.* 20 (2 Apr. 1948), pp. 367–387. DOI: 10.1103/RevModPhys.20.367. URL: <https://link.aps.org/doi/10.1103/RevModPhys.20.367>.

- [31] Yakir Aharonov, David Z. Albert, and Lev Vaidman. “How the result of a measurement of a component of the spin of a spin-1/2 particle can turn out to be 100”. In: *Phys. Rev. Lett.* 60 (14 Apr. 1988), pp. 1351–1354. DOI: 10.1103/PhysRevLett.60.1351. URL: <https://link.aps.org/doi/10.1103/PhysRevLett.60.1351>.
- [32] Justin Dressel et al. “Colloquium”. In: *Rev. Mod. Phys.* 86 (1 Mar. 2014), pp. 307–316. DOI: 10.1103/RevModPhys.86.307. URL: <https://link.aps.org/doi/10.1103/RevModPhys.86.307>.
- [33] Abraham G. Kofman, Sahel Ashhab, and Franco Nori. “Nonperturbative theory of weak pre- and post-selected measurements”. In: *Physics Reports* 520.2 (2012). Nonperturbative theory of weak pre- and post-selected measurements, pp. 43–133. ISSN: 0370-1573. DOI: <https://doi.org/10.1016/j.physrep.2012.07.001>. URL: <http://www.sciencedirect.com/science/article/pii/S0370157312002050>.
- [34] Travis Norsen and Ward Struyve. “Weak measurement and Bohmian conditional wave functions”. In: *Annals of Physics* 350 (2014), pp. 166–178. ISSN: 0003-4916. DOI: <https://doi.org/10.1016/j.aop.2014.07.014>. URL: <http://www.sciencedirect.com/science/article/pii/S0003491614001869>.
- [35] Reza Mir et al. “A double-slit ‘which-way’ experiment on the complementarity–uncertainty debate”. In: 9 (June 2007).
- [36] Konrad Banaszek. “Fidelity Balance in Quantum Operations”. In: *Phys. Rev. Lett.* 86 (7 Feb. 2001), pp. 1366–1369. DOI: 10.1103/PhysRevLett.86.1366. URL: <https://link.aps.org/doi/10.1103/PhysRevLett.86.1366>.
- [37] Y. Aharonov and L. Vaidman. “The Two-State Vector Formalism: An Updated Review”. In: *Lecture Notes in Physics, Berlin Springer Verlag*. Vol. 734. Lecture Notes in Physics, Berlin Springer Verlag, 2008, pp. 399–447. DOI: 10.1007/978-3-540-73473-4_13.
- [38] Yakir Aharonov and Lev Vaidman. “Properties of a quantum system during the time interval between two measurements”. In: *Phys. Rev. A* 41 (1 Jan. 1990), pp. 11–20. DOI: 10.1103/PhysRevA.41.11. URL: <https://link.aps.org/doi/10.1103/PhysRevA.41.11>.
- [39] Yakir Aharonov and Daniel Rohrlich. “Weak Values”. In: *Quantum Paradoxes*. Wiley-VCH Verlag GmbH, 2008, pp. 225–248. ISBN: 9783527619115. DOI: 10.1002/9783527619115.ch16. URL: <http://dx.doi.org/10.1002/9783527619115.ch16>.
- [40] Yakir Aharonov, Peter G. Bergmann, and Joel L. Lebowitz. “Time Symmetry in the Quantum Process of Measurement”. In: *Phys. Rev.* 134 (6B June 1964), pp. 1410–1416. DOI: 10.1103/PhysRev.134.B1410. URL: <https://link.aps.org/doi/10.1103/PhysRev.134.B1410>.
- [41] Y. Aharonov and A. Botero. “Quantum averages of weak values”. In: *Phys. Rev. Lett. A* 72.5, 052111 (Nov. 2005), p. 052111. DOI: 10.1103/PhysRevA.72.052111. eprint: [quant-ph/0503225](https://arxiv.org/abs/quant-ph/0503225).
- [42] A. J. Leggett. “Comment on “How the result of a measurement of a component of the spin of a spin-1/2 particle can turn out to be 100””. In: *Phys. Rev. Lett.* 62 (19 May 1989), pp. 2325–2325. DOI: 10.1103/PhysRevLett.62.2325. URL: <https://link.aps.org/doi/10.1103/PhysRevLett.62.2325>.
- [43] D. Dürr, S. Goldstein, and N. Zanghí. “On the Weak Measurement of Velocity in Bohmian Mechanics”. In: *Journal of Statistical Physics* 134 (Jan. 2009), pp. 1023–1032. DOI: 10.1007/s10955-008-9674-0.

- [44] Konstantin Y Bliokh et al. “Photon trajectories, anomalous velocities and weak measurements: a classical interpretation”. In: *New Journal of Physics* 15.7 (2013), p. 073022. URL: <http://stacks.iop.org/1367-2630/15/i=7/a=073022>.
- [45] T. Mori and I. Tsutsui. “Quantum trajectories based on the weak value”. In: *Progress of Theoretical and Experimental Physics* 2015.4, 043A01 (Apr. 2015), 043A01. DOI: 10.1093/ptep/ptv032. arXiv: 1412.0916 [quant-ph].
- [46] Sacha Kocsis et al. “Observing the Average Trajectories of Single Photons in a Two-Slit Interferometer”. In: *Science* 332.6034 (2011), pp. 1170–1173. ISSN: 0036-8075. DOI: 10.1126/science.1202218. URL: <http://science.sciencemag.org/content/332/6034/1170>.
- [47] Olaf Nairz, Markus Arndt, and Anton Zeilinger. “Quantum interference experiments with large molecules”. In: *American Journal of Physics* 71 (2003), p. 319. DOI: 10.1119/1.1531580.
- [48] Richard Feynman, Robert B. Leighton, and Matthew Sands. *Lectures on Physics*. Vol. 3. Addison Wesley, 1964.
- [49] Christopher Dewdney, L Hardy, and E.J. Squires. “How late measurements of quantum trajectories can fool a detector”. In: 184 (Dec. 1993), pp. 6–11.
- [50] B. E. A. Saleh and M. C. Teich. *Photon Optics*. Wiley-Blackwell, 1991. Chap. 6. ISBN: 9780471213741. DOI: 10.1002/0471213748.ch11. URL: <https://onlinelibrary.wiley.com/doi/abs/10.1002/0471213748.ch11>.
- [51] V. G. Dmitriev, G. G. Gurzadyan, and D. N. Nikogosyan. *Handbook of Nonlinear Optical Crystals. Second, revised and updated edition*. Springer. DOI: 10.1002/crat.2170320503. URL: <https://onlinelibrary.wiley.com/doi/abs/10.1002/crat.2170320503>.
- [52] J. H. Eberly, L. Mandel, and E. Wolf. “Coherence and Quantum Optics VII”. In: 1996, pp. 313–322. DOI: 10.1007/978-1-4757-9742-8.